# Diversity and Delay Analysis of Buffer–Aided BICM–OFDM Relaying

Toufiqul Islam, *Student Member, IEEE*, Aissa Ikhlef, *Member, IEEE*, Robert Schober, *Fellow, IEEE*, and Vijay K. Bhargava, *Fellow, IEEE*

***Abstract*—In this paper, we study a cooperative diversity scheme for wireless systems where the relay is equipped with a buffer. We consider practical frequency–selective channels and adopt the combination of bit interleaved coded modulation and orthogonal frequency division multiplexing (BICM–OFDM). We propose a novel link selection protocol for BICM–OFDM systems where the relay either transmits or receives in a given time slot depending on the quality of the links. We derive a closed–form upper bound for the asymptotic worst–case pairwise error probability (PEP) and the diversity gain of the considered buffer–aided relaying scheme for both infinite and finite buffer size. We show that significant diversity gains can be achieved with buffer–aided relaying compared to conventional relaying at the expense of larger packet delays. In fact, for buffers of infinite (or very large) size, the diversity gain is doubled for links with identical frequency diversity, and an even higher diversity gain advantage is possible for links with non–identical frequency diversities. Furthermore, we perform an exact closed–form average delay analysis for buffers of both finite and infinite size which provides important insight into the achieved delay–performance tradeoff. The derived analytical results and performance gains are corroborated by extensive simulation results.**

***Index Terms*—BICM, OFDM, Cooperative Diversity, Buffer–Aided Relaying.**

## I. Introduction

Cooperative diversity techniques can achieve high diversity gains in distributed wireless networks where nodes are allowed to cooperate by relaying each other's signal [1]. Conventional relay cooperation protocols rely on either amplify–and–forward (AF) or decode–and–forward (DF) operations [1] and the relay receives and re–transmits in successive time slots. In conventional relaying systems, the end–to–end performance is limited by the bottleneck relay link because the relay employs a fixed schedule for reception and transmission without considering the link quality. In this paper, we consider a network consisting of a source, a relay, and a destination, and we do not impose a fixed schedule, but adopt an adaptive schedule for reception and transmission at the relay. In particular, the relay receives (transmits) only when the source $S$ to relay $R$ (relay $R$ to destination $D$) link $S \to R$ ($R \to D$) is stronger compared to the $R \to D$ ($S \to R$) link. This is only possible if the relay is equipped with a buffer and can store packets before re–transmitting them later at a suitable time.

The buffer–aided relaying concept is comparatively new and the literature in this area is relatively sparse. Buffer–aided relaying protocols have been considered before in [2]–[9]. In [2], two buffer–aided relaying schemes were proposed where the relay receives for a fixed number of time slots and then re–transmits, and a throughput improvement was demonstrated compared to receiving and re–transmitting in subsequent time slots. The authors in [3] considered a joint cross–layer scheduling and relay selection problem where the relays were equipped with buffers and reported that considerable throughput improvements can be achieved compared to relaying without buffers. The authors in [4] found that, at the expense of a packet delay, the asymptotic throughput can be improved by considering relay buffering and relay mobility. In [5], it was shown that the throughput can be improved if the relay employs adaptive link selection, i.e., the relay receives (transmits) only when the $S \to R$ ($R \to D$) link enjoys a better quality than the $R \to D$ ($S \to R$) link. The authors in [6] applied adaptive link selection in two–way relay networks and considered sum–rate maximization. In [7], a relay selection scheme was proposed that takes into account the quality of the links and the status of the relay buffer of finite size. In [8], relay selection was considered and it was proposed to select the relays with the best $S \to R$ and the best $R \to D$ channels for reception and transmission, respectively. It was shown that this max–max relay selection criterion results in an improved coding gain but no additional diversity gain. Throughput and end–to–end delay analyses for relay selection in full–duplex relay networks with infinite buffer size were provided in [9]. We note that [2]– [6], [9] focused on throughput optimization for flat–fading links and [7], [8] considered performance analysis of buffer–aided relay selection for uncoded flat–fading links. Hence, the results in these papers are not directly applicable to practical systems with frequency–selective channels and channel coding with non–ideal interleaving. In this work, we adopt the combination of bit interleaved coded modulation and orthogonal frequency division multiplexing (BICM–OFDM) [10] to exploit the frequency diversity offered by the channel. We propose a link selection protocol suitable for BICM–OFDM and explore possible diversity gain benefits over conventional relaying without buffers. To the best of the authors' knowledge, an end–to–end error rate and delay analysis for buffer–aided relaying

Manuscript received September 3, 2012; revised March 16, 2013; accepted August 4, 2013. The review of this paper was coordinated by Prof. Shuangqing Wei. This work was supported in part by a Vanier Canada Graduate Scholarship. This work was presented in part at the IEEE Globecom, Anaheim, CA, December 2012.

Toufiqul Islam, Robert Schober, and Vijay K. Bhargava are with the Department of Electrical and Computer Engineering, The University of British Columbia, Vancouver, Canada. A. Ikhlef was with The University of British Columbia, Vancouver when this work was performed. Since June 2013 he has been with Toshiba Research Europe Limited, Bristol, UK (e-mail: {toufiq, aikhlef, rschober, vijayb}@ece.ubc.ca).

with link selection is not available in the literature yet, not even for uncoded flat–flading links, despite the promise of buffer–aided relaying.

In this paper, we present novel buffer–aided link selection protocols for BICM–OFDM based DF relaying with buffers of both infinite and finite sizes. We assume that the source has always data to transmit, i.e., it has an infinite backlog of information bits. Both source and relay adopt standard BICM–OFDM transmission. For buffers of infinite size, the relay receives (transmits) when the $S \rightarrow R$ ($R \rightarrow D$) link is stronger compared to the $R \rightarrow D$ ($S \rightarrow D$) link over a certain set of OFDM sub–carriers. We consider the general case where the links can be dissimilar in terms of average signal–to–noise ratio (SNR) and frequency diversity. The decision threshold for link selection is chosen such that the selection of both links is equally probable. For buffers of finite size, we adjust the transmission such that the $S \rightarrow R$ ($R \rightarrow D$) link is chosen when the buffer is empty (full), otherwise we revert to the link selection protocol based on channel quality. We study the worst–case pairwise probability (PEP) of the system, obtain a closed–form upper bound on the PEP for both finite and infinite buffer size, and derive the diversity gain of the system for infinite buffer size, which provides important insight into the maximum achievable diversity gain for the proposed link selection rule. In fact, we show that the diversity gain doubles and more than doubles compared to that of conventional DF relaying if both links have identical and non–identical frequency diversity, respectively, as the performance is no longer limited by the bottleneck link. For the practical case, when buffers of finite size are used, we observe impressive coding gains even with buffers of moderate size, if not any diversity gain. Our simulation results reveal that as the size of the buffer increases, the diversity gain gradually increases in the practical SNR region. As the performance gains come at the expense of a delay in the network, we also analyze the average end–to–end packet delay for both finite and infinite buffer size. In fact, our results reveal that the proposed scheme is suitable for applications that require high reliability but can tolerate delays.

*Notation:* In this paper, $\mathcal{E}\{\cdot\}$, $(\cdot)^T$, $(\cdot)^H$, and $|\cdot|$ denote statistical expectation, the transpose operation, the Hermitian operation, and the magnitude of a scalar or the cardinality of a set, respectively. $\lambda_m(\boldsymbol{X})$, $1 \leq m \leq \mathrm{rank}\{\boldsymbol{X}\}$, denote the non–zero eigenvalues of matrix $\boldsymbol{X}$, $\Gamma(\cdot)$ denotes the Gamma function, and EVD stands for Eigenvalue decomposition.

## II. System Model

The considered system consists of a source terminal $S$, one DF relay $R$ equipped with a buffer (cf. Fig. 1), and one destination terminal $D$. The direct link between $S$ and $D$ is not exploited due to heavy attenuation and/or simplicity of implementation. We assume that the transmission is organized in packets and the channels are constant for the duration of one packet and vary independently from one packet to the next (block fading model). We also assume that source $S$ has always data to transmit. For the relay, buffers of both finite and infinite sizes are considered. Though impractical, the analysis of buffers of infinite size provides significant insight into the achievable performance. The link selection protocol determines whether relay $R$ receives a packet from source $S$ or transmits a packet to destination $D$. In this paper, we assume that the link selection is performed at the destination node $D$. To this end, $D$ acquires the channel state information (CSI) of both the $S$–$R$ link and $R$–$D$ link, keeps track of the status of the buffer at $R$, selects the transmitting node based on the selection criterion proposed in Section II-B, and informs $S$ and $R$ about its decision via a low rate feedback link.We note that in this regard buffer–aided relaying introduces additional signalling overhead compared to conventional relaying where $D$ does not have to know the CSI of the $S$–$R$ link and no link selection results have to be fed back. We assume $S$ and $R$ transmit at a fixed rate determined by the adopted coding and modulation scheme. In the following, we present the signal model and the link selection criterion.

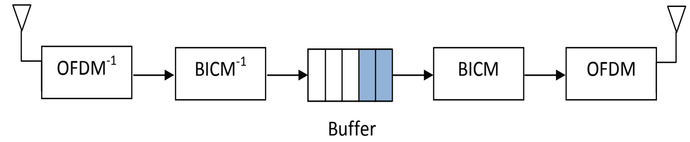


Fig. 1. Relay system model. “OFDM” and “OFDM$^{-1}$” represent Inverse Fast Fourier Transform (IFFT) followed by Cyclic Prefix (CP) insertion and CP rejection followed by FFT, respectively. “BICM” and “BICM$^{-1}$” represent channel coding followed by interleaving and modulation and bit metric calculation followed by de–interleaving and decoding, respectively. Each buffer element is assumed to store one packet of information bits. If the $R \rightarrow D$ link is selected, the content of the right most buffer element is transmitted, i.e., we adopt a First In First Out (FIFO) mode. Shaded buffer elements are full.

### A. Signal Model

Source $S$ employs conventional BICM–OFDM [10]. As usual, the BICM system comprises a binary encoder, a bit-interleaver, and a memoryless mapper, which maps blocks of $m$ interleaved bits to a signal constellation $\mathcal{X}$ comprising $|\mathcal{X}| = M = 2^m$ signal points [11]. We assume a convolutional encoder with minimum free distance $d_{\mathrm{f}}$ and adopt Gray mapping, which is customary in BICM systems [12]. The BICM block is followed by an OFDM modulator, cf. Fig. 1. We assume conventional OFDM processing at the source, the relay, and the destination and a sufficiently long cyclic prefix (CP) to avoid interference between sub–carriers. One OFDM symbol comprises $N_t$ sub–carriers of which $N < N_t$ are used to carry data. We assume coding and interleaving over one OFDM symbol. Thus, the $\log_2(M)N$ output bits of the convolutional encoder, $c_{k'}$, $0 \leq k' < \log_2(M)N$, are interleaved and mapped onto the $N$ data symbols $X[k] \in \mathcal{X}$, $k \in \mathcal{N}$, $\mathcal{N} \triangleq \{0, 1, \ldots, N-1\}$, belonging to one OFDM symbol. The data symbols have unit average energy, i.e., $\mathcal{E}\{|X[k]|^2\} = 1$. The effect of the interleaver can be modeled by the mapping $k' \rightarrow (k, i)$, where $k'$ denotes the original index of coded bit $c_{k'}$, and $k$ and $i$ denote the index of symbol $X[k]$ and the position of $c_{k'}$ in the label of $X[k]$, respectively. Assuming $d_{\mathrm{f}}$ distinct bits between any two codewords span at most $d > d_{\mathrm{f}}$ consecutive bits in the trellis, the adopted interleaver ensures that any two coded bits $c_{k'}$ and $c_{k'+u}$, $u > 0$, are assigned to different data symbols (and thus to different sub–carriers) if $u \leq d$.

If the $S \to R$ link is selected for transmission at time slot $t$, the signal received at $R$ from $S$ on the $k$th sub–carrier can be modeled as

$$Y_{SR}^{t}[k] = \sqrt{P_S} H_{SR}^{t}[k] X[k] + N_{SR}[k], \quad \forall j, k, \tag{1}$$

where $P_S$ denotes the average transmit power per sub–carrier at $S$, $N_{SR}[k]$ is complex additive white Gaussian noise (AWGN) with variance $N_0$, and $H_{SR}^{t}[k]$ is the gain of the $S \to R$ channel on sub–carrier $k$ at time $t$.

To decode the bits transmitted by $S$, $R$ computes the BICM bit metric for the $i$th bit in the label of symbol $X[k]$ as [11]

$$\zeta_k^i[c_{k'}] = \min_{X \in \mathcal{X}_{c_{k'}}^i} \left\{ |Y_{SR}^{t}[k] - \sqrt{P_S} H_{SR}^{t}[k] X|^2 \right\}, \tag{2}$$

where $\mathcal{X}_b^i$ denotes the subset of all symbols $X \in \mathcal{X}$ whose label has value $b \in \{0, 1\}$ in position $i$. The bit metrics are de–interleaved and Viterbi decoded at $R$.

Similarly, if the $R \to D$ link is selected for transmission at time slot $q > t$, the signal received at $D$ from $R$ on the $k$th sub–carrier can be modeled as

$$Y_{RD}^{q}[k] = \sqrt{P_R} H_{RD}^{q}[k] X'[k] + N_{RD}[k], \quad k \in \mathcal{N}, \tag{3}$$

where $P_R$ denotes the average transmit power per sub–carrier at $R$, $N_{RD}[k]$ is complex AWGN with variance $N_0$, and $H_{RD}^{q}[k]$ is the frequency response of the $R \to D$ channel. We assume that the relay adds the decoded source packet to the queue in its buffer regardless of whether it has been decoded correctly or not (cf. Fig. 1). [1] Thus, $X'[k]$ can be modeled as $X'[k] \in \{X[k], \hat{X}[k]\}$, where $\hat{X}[k] \neq X[k]$ denotes a decoded symbol in error. The destination computes the BICM bit metric in a similar fashion as in (2).

We do not consider power allocation in this paper. Hence, without loss of generality, we assume equal transmit powers at source and relay, $P_S = P_R = P$. At time $t$, the frequency response $H_Z^t[k]$, $Z \in \{SR, RD\}$, can be expressed as $H_Z^t[k] = \boldsymbol{w}_Z^H[k] \boldsymbol{P}_Z \boldsymbol{h}_Z^t$, where $\boldsymbol{w}_Z[k]$ is the discrete Fourier transform vector of length $L_Z$ on sub–carrier $k$, $\boldsymbol{P}_Z = \boldsymbol{C}_Z^{1/2}$ is the power delay profile matrix, $\boldsymbol{C}_Z = \mathcal{E}\{\boldsymbol{h}_Z^t \boldsymbol{h}_Z^{t\,H}\}$ is the full rank channel correlation matrix, $\boldsymbol{h}_Z^t$ is a vector of length $L_Z$ containing the channel impulse response (CIR) coefficients of link $Z$, and $L_Z$ is the CIR length of link $Z$ which is identical to the frequency diversity of link $Z$. Furthermore, we introduce the instantaneous sub–carrier SNRs of the $S \to R$ and $R \to D$ links at time $t$ as $\gamma_{SR}^t[k] \triangleq P_S |H_{SR}^t[k]|^2 / N_0 = \bar{\gamma} |H_{SR}^t[k]|^2$ and $\gamma_{RD}^t[k] \triangleq \bar{\gamma} |H_{RD}^t[k]|^2$, respectively, where $\bar{\gamma} \triangleq P/N_0$ denotes the transmit SNR. We define the average SNRs as $\bar{\gamma}_{SR} \triangleq \bar{\gamma} \mathcal{E}\{|H_{SR}^t[k]|^2\} = \bar{\gamma} \sigma_{h_{SR}}^2$ and $\bar{\gamma}_{RD} \triangleq \bar{\gamma} \mathcal{E}\{|H_{RD}^t[k]|^2\} = \bar{\gamma} \sigma_{h_{RD}}^2$. We assume $\sigma_{h_Z}^2 = d_Z^{-\alpha}$, where $d_Z$ is the length of link $Z$ and $\alpha$ is the path–loss exponent.

[1] We note that alternatively the relay could perform error detection (using e.g. a cyclic redundancy check (CRC) code) and request a packet retransmission if a packet is detected in error. In this case, the relay has to inform both source and destination about the retransmission via feedback channels, which increases the signalling overhead. Nevertheless, the investigation of the error performance, the delay, and an appropriate link selection criterion for this alternative transmission scheme is an interesting topic for future work. Other work that has considered DF relaying without error detection includes [13].

### B. Link Selection Criterion

In conventional AF and DF BICM–OFDM relaying, performance is limited by the bottleneck relay link and the diversity order is given by $\min(d_{\mathrm{f}}, L_{SR}, L_{RD})$ [14]. For example, if $d_{\mathrm{f}}$ is large enough and $L_{SR} < L_{RD}$, the $S \to R$ link frequency diversity limits the overall diversity gain and performance. To alleviate this problem, we equip the relay with a buffer to store packets sent by the source. The relay transmits (receives) only when the $R \to D$ ($S \to R$) link is better compared to the $S \to R$ ($R \to D$) link. In this section, we introduce a criterion for link selection suitable for BICM–OFDM. Note that the link selection criteria presented in [5], [15], [16] to improve the throughput performance for adaptive/fixed rate transmission are fundamentally different from our criterion, as the former were conceived for flat fading and capacity maximization. Below we present the proposed criterion for finite buffer size and discuss operation for infinite buffer size as a special case.

At high SNR, the performance of BICM–OFDM systems is limited by the worst–case error event, i.e., where two codewords differ only in $d_{\mathrm{f}}$ positions [10]. Since convolutional codes are trellis based, $d_{\mathrm{f}}$ distinct error bits appear in a finite number of consecutive trellis branches. By appropriate interleaver design, those $d_{\mathrm{f}}$ bits are mapped to $d_{\mathrm{f}}$ different sub–carriers[2]. For both the $S \to R$ and the $R \to D$ links, we explore all possible sets of $d_{\mathrm{f}}$ sub–carriers and determine the worst–case set for link $Z$ for time slot $t$ as

$$\mathcal{K}_{Z,t} = \arg \min_{\mathcal{K}_{d_{\mathrm{f}}} \subset \mathcal{K}} \sum_{k \in \mathcal{K}_{d_{\mathrm{f}}}} \gamma_Z^t[k], \; Z \in \{SR, RD\}, \tag{4}$$

where $\mathcal{K}$ is the ensemble set of all feasible sets of $d_{\mathrm{f}}$ sub–carriers, $\mathcal{K}_{d_{\mathrm{f}}}$ is a particular set of $d_{\mathrm{f}}$ sub–carriers belonging to $\mathcal{K}$, and $\mathcal{K}_{Z,t}$ denotes the set of sub–carriers which correspond to the worst–case error event for link $Z$ in time slot $t$. Now, we define $\gamma_Z^t = \sum_{k \in \mathcal{K}_{Z,t}} \gamma_Z^t[k]$, which is the sum of the instantaneous sub–carrier SNRs of link $Z$ corresponding to the worst–case sub–carrier set $\mathcal{K}_{Z,t}$. Note that the worst–case sets of the $S \to R$ and $R \to D$ links are in general different as the links fade independently. Now, we are ready to formulate the link selection criterion for the considered BICM–OFDM relaying scheme.

We assume that the buffer has $J$ elements and each element can store one packet of information bits. We denote $N_{\mathrm{f}}$ as the number of buffer elements which are full. For $0 < N_{\mathrm{f}} < J$, the $S \to R$ link is selected for transmission at time slot $t$ if

$$\gamma_{SR}^t \geq \rho \gamma_{RD}^t. \tag{5}$$

Here, $\rho$ is a decision threshold to ensure proper balance in selecting the $S \to R$ and $R \to D$ links. This is necessary because the $S \to R$ and $R \to D$ links may be non–identically distributed with average SNRs $\bar{\gamma}_{SR}$ and $\bar{\gamma}_{RD}$, respectively. The choice of $\rho$ will be discussed later. The criterion basically decides in favor of the $S \to R$ link if it is relatively stronger than the $R \to D$ link over the worst–case set of sub–carriers. Otherwise, the $R \to D$ link is selected. The link selection

[2] We assume non–ideal interleaving, i.e., interleaving within one OFDM symbol is considered.

TABLE I
LINK SELECTION PROTOCOL. X MEANS THAT LINK QUALITY DOES NOT AFFECT LINK SELECTION IN THE CORRESPONDING CASES.

| Case | Buffer state | Link quality | Selected link |
|---|---|---|---|
| 1 | $N_{\rm f}=0$ | X | $S\to R$ |
| 2 | $N_{\rm f}=J$ | X | $R\to D$ |
| 3 | $N_{\rm f}\neq\{0,J\}$ | $\gamma_{SR}^t\geq\rho\gamma_{RD}^t$ | $S\to R$ |
| 4 | $N_{\rm f}\neq\{0,J\}$ | $\gamma_{SR}^t<\rho\gamma_{RD}^t$ | $R\to D$ |

criterion described in (5) may not be suitable for $N_{\rm f}=\{0,J\}$ since a buffer can run empty (full) if the $R\to D$ ($S\to R$) link is repeatedly selected. To overcome this problem, we adjust the link selection criterion by taking into account the status of the buffer. Hence, we select the $S\to R$ link if $N_{\rm f}=0$, regardless of the quality of the $S\to R$ link. Similarly, the $R\to D$ link is selected if $N_{\rm f}=J$. Note that $J=1$ corresponds to conventional DF relaying where the relay receives and transmits in successive time slots, i.e., storing data over multiple time slots is not possible. A summary of the proposed link selection protocol is shown in Table I.[3]

## III. PEP AND DIVERSITY ANALYSIS

In this section, we derive an upper bound on the asymptotic worst–case PEP for BICM–OFDM with adaptive link selection for finite buffer size. Then, we obtain an upper bound for infinite buffer size as a special case. We also provide expressions for the maximum diversity order achievable with finite and infinite buffer size.

### A. Asymptotic PEP

We denote the transmitted codeword by $\boldsymbol{c}$ and the detected codewords at the relay and the destination by $\hat{\boldsymbol{c}}$ and $\tilde{\boldsymbol{c}}$, respectively. For a code with free distance $d_{\rm f}$, $\boldsymbol{c}_j$ and $\hat{\boldsymbol{c}}_j$ differ in $d_{\rm f}$ positions for the worst–case error event. We denote the subset of sub–carriers containing the $d_{\rm f}$ erroneous bits by $\mathcal{K}_{SR,t}$ when the $S\to R$ link is selected at time $t$. Similarly, if the $R\to D$ link is selected at time $q$ and $\hat{\boldsymbol{c}}$ and $\tilde{\boldsymbol{c}}$ form the worst–case error event, the subset of sub–carriers containing the $d_{\rm f}$ erroneous bits is denoted by $\mathcal{K}_{RD,q}$.

We analyze the worst–case PEP for $\overline{\gamma}_{SR},\overline{\gamma}_{RD}\to\infty$. Note that a codeword is received in error at $D$ if a) the $S\to R$ link causes an error and the $R\to D$ link is error free, b) $R$ receives the codeword correctly but the $R\to D$ link causes an error, and c) both links cause errors but the errors do not cancel each other. Assuming a code with free distance $d_{\rm f}$, the end–to–end worst–case PEP of two codewords $\boldsymbol{c}$ and $\tilde{\boldsymbol{c}}$ can be formulated as

$$\begin{aligned}P(\boldsymbol{c},\tilde{\boldsymbol{c}})\leq P_R(\boldsymbol{c},\hat{\boldsymbol{c}})(1-P_D(\hat{\boldsymbol{c}},\tilde{\boldsymbol{c}}))+P_D(\hat{\boldsymbol{c}},\tilde{\boldsymbol{c}})(1-P_R(\boldsymbol{c},\hat{\boldsymbol{c}}))\\ +P_R(\boldsymbol{c},\hat{\boldsymbol{c}})P_D(\hat{\boldsymbol{c}},\tilde{\boldsymbol{c}})\doteq P_R(\boldsymbol{c},\hat{\boldsymbol{c}})+P_D(\hat{\boldsymbol{c}},\tilde{\boldsymbol{c}}),\end{aligned}\tag{6}$$

where $P_R(\boldsymbol{c},\hat{\boldsymbol{c}})$ and $P_D(\hat{\boldsymbol{c}},\tilde{\boldsymbol{c}})$ denote the worst–case PEPs of the $S\to R$ and $R\to D$ links, respectively, and " $\doteq$ " denotes asymptotic equivalence.

At time slot $t$, the worst–case PEP of a link $Z$ conditioned on $\gamma_Z^t$ (cf. Section II-B) can be upper bounded as [10]

$$P(e|\gamma_Z^t)\leq\exp(-\eta\gamma_Z^t),\tag{7}$$

where $\eta\triangleq d_{\min}^2/(4N_0)$, and $d_{\min}$ is the minimum distance of the constellation $\mathcal{X}$.

Depending on the states of the buffer, we distinguish four cases for transmission of a source packet from $S$ to $D$. We denote the worst–case error probabilities for the different cases as $P_i$, $i\in\{1,\ldots,4\}$. $P_i$ depends on the probabilities of the buffer being full and empty, which are denoted by $P_{\rm full}$ and $P_{\rm empty}$, and the worst–case PEPs for the $S\to R$ and $R\to D$ links for the considered case, which are denoted by $P_R^i(\boldsymbol{c},\hat{\boldsymbol{c}})$ and $P_D^i(\hat{\boldsymbol{c}},\tilde{\boldsymbol{c}})$, respectively. Expressions for $P_{\rm full}$ and $P_{\rm empty}$ are derived in Appendix A. We study now the worst–case error probabilities for the four considered cases.

**Case** 1: In this case, we assume that the $S\to R$ and the $R\to D$ links are selected based on the link selection protocol in (5). Hence, the buffer is neither full nor empty. The joint probability of this event is $(1-P_{\rm empty})(1-P_{\rm full})$. We obtain $P_1$ as

$$P_1=(1-P_{\rm empty})(1-P_{\rm full})(P_R^1(\boldsymbol{c},\hat{\boldsymbol{c}})+P_D^1(\hat{\boldsymbol{c}},\tilde{\boldsymbol{c}})).\tag{8}$$

Now, based on the link selection criterion for $0<N_f<J$, $P_R^1(\boldsymbol{c},\hat{\boldsymbol{c}})$ and $P_D^1(\hat{\boldsymbol{c}},\tilde{\boldsymbol{c}})$ can be expressed as

$$\begin{aligned}P_R^1(\boldsymbol{c},\hat{\boldsymbol{c}})&\leq\mathcal{E}\{\exp(-\eta\gamma_{SR}^t)|\gamma_{SR}^t>\rho\gamma_{RD}^t\}\\&=\frac{\mathcal{E}\{\exp(-\eta\gamma_{SR}^t)\cap\gamma_{SR}^t>\rho\gamma_{RD}^t\}}{\Pr(\gamma_{SR}^t>\rho\gamma_{RD}^t)}\end{aligned}\tag{9}$$

$$\begin{aligned}P_D^1(\hat{\boldsymbol{c}},\tilde{\boldsymbol{c}})&\leq\mathcal{E}\{\exp(-\eta\gamma_{RD}^q)|\gamma_{RD}^q>\gamma_{SR}^q/\rho\}\\&=\frac{\mathcal{E}\{\exp(-\eta\gamma_{RD}^q)\cap\gamma_{RD}^q>\gamma_{SR}^q/\rho\}}{\Pr(\gamma_{RD}^q>\gamma_{SR}^q/\rho)},\end{aligned}\tag{10}$$

where $q>t$, $p\in\{t,q\}$. For the rest of the analysis, we drop the time index for brevity.In the following *Lemma*, we provide asymptotic upper bounds for $P_R^1(\boldsymbol{c},\hat{\boldsymbol{c}})$ and $P_D^1(\hat{\boldsymbol{c}},\tilde{\boldsymbol{c}})$.

*Lemma 1:* For $e\overline{\gamma}_{SR}=f\overline{\gamma}_{RD}=\overline{\gamma}_b\to\infty$, an asymptotic upper bound for $P_R^1(\boldsymbol{c},\hat{\boldsymbol{c}})$ and $P_D^1(\hat{\boldsymbol{c}},\tilde{\boldsymbol{c}})$ can be obtained as

$$P_R^1(\boldsymbol{c},\hat{\boldsymbol{c}})\leq\frac{\theta_{SR}}{\overline{\gamma}_b^{r_{SR}+r_{RD}}}\tag{11}$$

$$P_D^1(\hat{\boldsymbol{c}},\tilde{\boldsymbol{c}})\leq\frac{\theta_{RD}}{\overline{\gamma}_b^{r_{SR}+r_{RD}}},\tag{12}$$

respectively, where $r_Z\triangleq\min(d_{\rm f},L_Z)$ and the SNR-independent constants $\theta_{SR}$ and $\theta_{RD}$ are, respectively, given in (13) and (14) at the top of next page, where $\boldsymbol{B}_Z\triangleq\boldsymbol{P}_Z\boldsymbol{A}_Z\boldsymbol{P}_Z$ and $\boldsymbol{A}_Z=\sum_{k\in\mathcal{K}_Z}\boldsymbol{w}_Z[k]\boldsymbol{w}_Z^H[k]$.

*Proof:* Please refer to Appendix B. ∎

**Case** 2: In this case, the $S\to R$ link is selected since the buffer is empty. The decoded packet is transmitted at a later time by selecting the $R\to D$ link when the buffer is full. The joint probability of this event is $P_{\rm empty}P_{\rm full}$. We obtain $P_2$ as

$$P_2=P_{\rm empty}P_{\rm full}(P_R^2(\boldsymbol{c},\hat{\boldsymbol{c}})+P_D^2(\hat{\boldsymbol{c}},\tilde{\boldsymbol{c}})),\tag{15}$$

[3]We note that the proposed protocol can be refined by combining it with adaptive coding and modulation. In particular, since the destination has the CSI of both the $S$–$R$ and the $R$–$D$ links, it can select a coding and modulation scheme appropriate for the SNR of the selected link and feed this information back to the transmitting node. However, such a more sophisticated adaptive rate protocol will lead to a more involved performance and delay analysis and is left for future work.

$$\theta_{SR} = \frac{\Gamma(r_{SR}+r_{RD})}{\Pr(\gamma_{SR} > \rho\gamma_{RD}) r_{RD}\Gamma(r_{SR})\Gamma(r_{RD})\rho^{r_{RD}}\eta^{r_{SR}+r_{RD}}\left[\prod_{j=1}^{r_{SR}}\lambda_j(\boldsymbol{B}_{SR})\right]\left[\prod_{i=1}^{r_{RD}}\lambda_i(\boldsymbol{B}_{RD})\right]} \tag{13}$$

$$\theta_{RD} = \frac{\Gamma(r_{SR}+r_{RD})\rho^{r_{SR}}}{\Pr(\gamma_{RD} > \gamma_{SR}/\rho) r_{SR}\Gamma(r_{SR})\Gamma(r_{RD})\eta^{r_{SR}+r_{RD}}\left[\prod_{j=1}^{r_{SR}}\lambda_j(\boldsymbol{B}_{SR})\right]\left[\prod_{i=1}^{r_{RD}}\lambda_i(\boldsymbol{B}_{RD})\right]} \tag{14}$$

where $P_R^2(\boldsymbol{c},\hat{\boldsymbol{c}})$ and $P_D^2(\hat{\boldsymbol{c}},\tilde{\boldsymbol{c}}))$ are given by

$$P_R^2(\boldsymbol{c},\hat{\boldsymbol{c}}) \le \mathcal{E}\{\exp(-\eta\gamma_{SR})\} \tag{16}$$

$$P_D^2(\hat{\boldsymbol{c}},\tilde{\boldsymbol{c}}) \le \mathcal{E}\{\exp(-\eta\gamma_{RD})\}. \tag{17}$$

As link selection is not possible, we do not have the conditioning on the link SNRs in (16) and (17). Now, following [10], asymptotic upper bounds for $P_R^2(\boldsymbol{c},\hat{\boldsymbol{c}})$ and $P_D^2(\hat{\boldsymbol{c}},\tilde{\boldsymbol{c}})$ are given by

$$P_R^2(\boldsymbol{c},\hat{\boldsymbol{c}}) \le \frac{1}{(\eta\bar{\gamma}_{SR})^{r_{SR}}\prod_{i=1}^{r_{SR}}\lambda_i(\boldsymbol{B}_{SR})} = \frac{\nu_{SR}}{\bar{\gamma}_{SR}^{r_{SR}}} \tag{18}$$

$$P_D^2(\hat{\boldsymbol{c}},\tilde{\boldsymbol{c}}) \le \frac{1}{(\eta\bar{\gamma}_{RD})^{r_{RD}}\prod_{i=1}^{r_{RD}}\lambda_i(\boldsymbol{B}_{RD})} = \frac{\nu_{RD}}{\bar{\gamma}_{RD}^{r_{RD}}}, \tag{19}$$

where $\nu_Z \triangleq 1/(\eta^{r_Z}\prod_{i=1}^{r_Z}\lambda_i(\boldsymbol{B}_Z))$, $Z\in\{SR,RD\}$.

**Case** 3: In this case, we assume that when the packet was transmitted from $S$, the buffer was empty. Hence, the $S\to R$ link is selected regardless of the quality of the link. However, the buffer is not full when the $R\to D$ link is selected based on the link selection criterion. The joint probability of this event is $P_{\text{empty}}(1-P_{\text{full}})$. We obtain $P_3$ as

$$P_3 = P_{\text{empty}}(1-P_{\text{full}})(P_R^3(\boldsymbol{c},\hat{\boldsymbol{c}}) + P_D^3(\hat{\boldsymbol{c}},\tilde{\boldsymbol{c}})), \tag{20}$$

where $P_R^3(\boldsymbol{c},\hat{\boldsymbol{c}}) = P_R^2(\boldsymbol{c},\hat{\boldsymbol{c}})$ and $P_D^3(\hat{\boldsymbol{c}},\tilde{\boldsymbol{c}}) = P_D^1(\hat{\boldsymbol{c}},\tilde{\boldsymbol{c}})$.

**Case** 4: In this case, we assume that the packet was transmitted from $S$ via link selection, i.e., the buffer was not empty. However, when the packet was re–transmitted by $R$, the buffer was full. Hence, the $R\to D$ link is selected regardless of the link quality. The joint probability of this event is $(1-P_{\text{empty}})P_{\text{full}}$. We obtain $P_4$ as

$$P_4 = (1-P_{\text{empty}})P_{\text{full}}(P_R^4(\boldsymbol{c},\hat{\boldsymbol{c}}) + P_D^4(\hat{\boldsymbol{c}},\tilde{\boldsymbol{c}})), \tag{21}$$

where $P_R^4(\boldsymbol{c},\hat{\boldsymbol{c}}) = P_R^1(\boldsymbol{c},\hat{\boldsymbol{c}})$ and $P_D^4(\hat{\boldsymbol{c}},\tilde{\boldsymbol{c}})) = P_D^2(\hat{\boldsymbol{c}},\tilde{\boldsymbol{c}})$.

As the four cases are disjoint, we obtain the end–to–end asymptotic PEP, $P^{FB}(\boldsymbol{c},\tilde{\boldsymbol{c}})$, as $P^{FB}(\boldsymbol{c},\tilde{\boldsymbol{c}}) = \sum_{i=1}^4 P_i$ and assuming $e\bar{\gamma}_{SR} = f\bar{\gamma}_{RD} = \bar{\gamma}_b \to \infty$, an asymptotic upper bound on $P^{FB}(\boldsymbol{c},\tilde{\boldsymbol{c}})$ is given by

$$\begin{aligned} P^{FB}(\boldsymbol{c},\tilde{\boldsymbol{c}}) \le{}& (1-P_{\text{empty}})(1-P_{\text{full}})\frac{\theta_{SR}+\theta_{RD}}{\bar{\gamma}_b^{r_{SR}+r_{RD}}} \\ &+ P_{\text{empty}}P_{\text{full}}\Big(\frac{\nu_{SR}}{\bar{\gamma}_b^{r_{SR}}} + \frac{\nu_{RD}}{\bar{\gamma}_b^{r_{RD}}}\Big) \\ &+ P_{\text{empty}}(1-P_{\text{full}})\Big(\frac{\nu_{SR}}{\bar{\gamma}_b^{r_{SR}}} + \frac{\theta_{RD}}{\bar{\gamma}_b^{r_{SR}+r_{RD}}}\Big) \\ &+ (1-P_{\text{empty}})P_{\text{full}}\Big(\frac{\theta_{SR}}{\bar{\gamma}_b^{r_{SR}+r_{RD}}} + \frac{\nu_{RD}}{\bar{\gamma}_b^{r_{RD}}}\Big). \end{aligned} \tag{22}$$

*Remark* 1: For finite buffer size, we observe that the lowest rate at which the PEP $P^{FB}(\boldsymbol{c},\tilde{\boldsymbol{c}})$ decays is $\min(r_{SR},r_{RD})$. To observe the maximum decaying rate $r_{SR}+r_{RD}$, we must have $P_{\text{empty}}, P_{\text{full}} \to 0$ as $J\to\infty$, which makes the first term in the sum in (22) dominant. For this reason, the choice of $\rho$ is critical. Note that for buffers of finite size, the suitable choice of $\rho$ depends on how $P_{\text{empty}}$ and $P_{\text{full}}$ behave as $J\to\infty$, given the probabilities of selecting the $S\to R$ and $R\to D$ links, i.e., $P_{SR}$ and $P_{RD}$, respectively. The following *Lemma* specifies how $P_{\text{empty}}, P_{\text{full}} \to 0$ can be achieved..

*Lemma 2:* For $\zeta \triangleq \frac{P_{RD}}{P_{SR}} = 1$, $P_{\text{empty}}, P_{\text{full}} \to 0$ when $J\to\infty$.

*Proof:* Please refer to Appendix D. ∎

Note that for $P_{SR} = P_{RD} = \frac{1}{2}$, $P_{\text{empty}} = P_{\text{full}} = 1/(2J)$ holds from (41). From *Lemma* 2, we observe that the choice of $\rho$ must ensure that the selection of the $S\to R$ and $R\to D$ links is equally probable, i.e.,

$$\rho = \frac{\mathcal{E}\{\gamma_{SR}\}}{\mathcal{E}\{\gamma_{RD}\}} \tag{23}$$

holds. Recall from Section II-A that $\gamma_Z = \bar{\gamma}\sum_{i=1}^{r_Z}\lambda_i(\boldsymbol{B}_Z)|v_Z(i)|^2$, i.e., $\mathcal{E}\{\gamma_Z\} = \bar{\gamma}\sigma_{h_Z}^2\sum_{i=1}^{r_Z}\lambda_i(\boldsymbol{B}_Z) = \bar{\gamma}_Z\sum_{i=1}^{r_Z}\lambda_i(\boldsymbol{B}_Z)$. Hence, we obtain $\rho$ from (23) as

$$\rho = \frac{\bar{\gamma}_{SR}\sum_{i=1}^{r_{SR}}\lambda_i(\boldsymbol{B}_{SR})}{\bar{\gamma}_{RD}\sum_{j=1}^{r_{RD}}\lambda_j(\boldsymbol{B}_{RD})}. \tag{24}$$

For $\rho$ chosen as in (24) and very large values of $J$ (ideally $J\to\infty$), we obtain

$$P^{FB}(\boldsymbol{c},\tilde{\boldsymbol{c}}) \le \frac{\theta_{SR}+\theta_{RD}}{\bar{\gamma}_b^{r_{SR}+r_{RD}}}, \tag{25}$$

where the maximum decaying rate of $r_{SR}+r_{RD}$ is observed.

**Special Case**: *Uniform Power Delay Profile*

Further simplification is possible for $\rho$ presented in (24). In fact, we observe that if a uniform power delay profile (PDP) is adopted, $\rho$ in (24) becomes independent of the frequency diversity of the links. It can be easily shown that $\sum_{i=1}^{r_Z}\lambda_i(\boldsymbol{A}_Z) = d_{\text{f}}L_Z$ (cf. (52))[4] because of the linearity of the trace of matrices, $\text{trace}(\sum_i \boldsymbol{U}_i) = \sum_i \text{trace}(\boldsymbol{U}_i)$. By adopting a uniform PDP $\boldsymbol{P}_Z$, we obtain $\sum_{i=1}^{r_Z}\lambda_i(\boldsymbol{B}_Z) = d_{\text{f}}$ which is independent of the frequency diversity of the links. In that case, $\rho$ simplifies to

$$\rho = \frac{\bar{\gamma}_{SR}}{\bar{\gamma}_{RD}} = \frac{\sigma_{h_{SR}}^2}{\sigma_{h_{RD}}^2}. \tag{26}$$

Note that if the links are identically distributed with equal variance (i.e., the link distances $d_{SR} = d_{RD}$ are identical),

[4]Note that $\text{trace}(\boldsymbol{U}) = \sum_i \lambda_i(\boldsymbol{U})$. Now $\text{trace}(\sum_{k\in\mathcal{K}_Z}\boldsymbol{w}_Z[k]\boldsymbol{w}_Z^H[k]) = \sum_{k\in\mathcal{K}_Z}\text{trace}(\boldsymbol{w}_Z[k]\boldsymbol{w}_Z^H[k]) = d_{\text{f}}L_Z$ holds as $|\mathcal{K}_Z| = d_{\text{f}}$ and $\boldsymbol{w}_Z[k]\boldsymbol{w}_Z^H[k]$ is a rank one matrix with a single non–zero eigenvalue given by $\boldsymbol{w}_Z^H(k)\boldsymbol{w}_Z(k) = L_Z$.

$\rho = 1$ is valid.

On the other hand, it is also insightful to study the achievable performance of relaying with a buffer of infinite size. Below, based on (22), we obtain the PEP for a buffer with infinite size as a special case.

**Infinite Buffer Size**

In case of buffers with infinite size, $P_{\text{full}} = 0$. However, if $N_{\text{f}} = 0$, we have no other choice but to select the $S \rightarrow R$ link. We can avoid reaching the empty buffer state by careful selection of the decision threshold $\rho$. Here, we have two possible cases: Cases 1 and 3 discussed for finite buffer size. From (22), we obtain an upper bound on the PEP for infinite buffer size as

$$P^{IB}(\boldsymbol{c}, \tilde{\boldsymbol{c}}) \leq (1 - P_{\text{empty}}) \frac{\theta_{SR} + \theta_{RD}}{\bar{\gamma}_b^{r_{SR}+r_{RD}}} + P_{\text{empty}} \Big( \frac{\nu_{SR}}{\bar{\gamma}_b^{r_{SR}}} + \frac{\theta_{RD}}{\bar{\gamma}_b^{r_{SR}+r_{RD}}} \Big). \quad (27)$$

From (27), we observe that the maximum decaying rate $r_{SR} + r_{RD}$ can be achieved if $P_{\text{empty}} = 0$. Hence, we have to find allowable values for $\rho$ such that $P_{\text{empty}} = 0$ holds.

For infinite buffer size, we observe in view of *Lemma* 2 for $P_{SR} > P_{RD}$ (cf. Case 3 in Appendix D) that any $\rho \leq \frac{\mathcal{E}\{\gamma_{SR}\}}{\mathcal{E}\{\gamma_{RD}\}}$ ensures $P_{\text{empty}} = 0$ as the $S \rightarrow R$ link is selected more often on average. Selecting $\rho$ in this manner, we obtain

$$P^{IB}(\boldsymbol{c}, \tilde{\boldsymbol{c}}) \leq \frac{\theta_{SR} + \theta_{RD}}{\bar{\gamma}_b^{r_{SR}+r_{RD}}}. \quad (28)$$

*Remark* 2: We observe that $\rho$ chosen as in (24) ensures that $P_{\text{empty}}, P_{\text{full}} \rightarrow 0$ for very large buffer sizes. Thus, $P^{FB}(\boldsymbol{c}, \tilde{\boldsymbol{c}})|_{J \rightarrow \infty}$ converges to $P^{IB}(\boldsymbol{c}, \tilde{\boldsymbol{c}})$ in (28).

*Remark* 3: The link selection rule presented in (5) establishes a virtual $R \rightarrow D$ link with average SNR $\rho\bar{\gamma}_{RD}$. Choosing $\rho$ according to (24), which makes the $S \rightarrow R$ and the virtual $R \rightarrow D$ links identically distributed if the same PDP is assumed for both links, ensures that the links are selected with equal probability. When $\bar{\gamma}_{SR} \neq \bar{\gamma}_{RD}$, the rule in (5) is not equivalent to selecting the link according to $\max_{Z \in \{SR,RD\}} \ \gamma_Z$ (which corresponds to $\rho = 1$ in (5)), where the latter criterion always chooses the best link according to the instantaneous SNR $\gamma_Z$. However, adopting $\rho = 1$ is, in general, not a wise choice. To demonstrate this, we consider two simple examples for the uniform PDP. Firstly, when $\bar{\gamma}_{RD} > \bar{\gamma}_{SR}$, for $\rho = 1$, the $R \rightarrow D$ link is selected more often on average, and there is a high probability that the buffer will be empty most of the time. Then, the relay will have no other choice but to receive packets from the source even if the $S \rightarrow R$ link quality is poor, which causes a potential diversity loss. Secondly, when $\bar{\gamma}_{SR} > \bar{\gamma}_{RD}$, for $\rho = 1$, the $S \rightarrow R$ link will be selected more often resulting in an increase of the size of the buffer queue and hence it will take a long time for the packets to reach the destination. As buffer overflow never occurs with infinite buffer size, $\rho = 1$ selects the best link and is expected to perform better compared to the choice of $\rho$ in (26). In this case, adopting $\rho$ in (26) enhances the quality of the virtual $R \rightarrow D$ link such that the links are selected with equal probability and the overall delay performance improves. In conclusion, choosing $\rho$ according to (24) / (26) provides a profitable tradeoff between performance and system delay. In Section V, we compare the performance for $\rho = 1$ and $\rho$ in (26) for both $\bar{\gamma}_{SR} < \bar{\gamma}_{RD}$ and $\bar{\gamma}_{SR} > \bar{\gamma}_{RD}$.

### B. Diversity Gain

We define the diversity gain as the negative slope of the asymptotic PEP as a function of $\bar{\gamma}_b$ on a double–logarithmic scale. Thus, based on (28), the diversity gain with infinite buffer size for $\rho \leq \frac{\mathcal{E}\{\gamma_{SR}\}}{\mathcal{E}\{\gamma_{RD}\}}$ is given by

$$G_d = r_{SR} + r_{RD} = \min\{d_{\text{f}}, L_{SR}\} + \min\{d_{\text{f}}, L_{RD}\}. \quad (29)$$

For conventional DF [14] and AF [17] BICM–OFDM relaying schemes, we have $G_d^{\text{AF/DF}} = \min\{d_{\text{f}}, L_{SR}, L_{RD}\}$. Hence, by adopting a code with sufficiently large $d_{\text{f}}$, remarkable diversity gains can be observed with buffer–aided relaying. If the links possess identical frequency diversity, i.e., $L_{SR} = L_{RD}$, then $G_d = 2G_d^{\text{AF/DF}}$ holds. On the other hand, if the frequency diversities of the links are not identical, i.e., $L_{SR} \neq L_{RD}$, then $G_d > 2G_d^{\text{AF/DF}}$ is valid because the diversity gain for buffer–aided relaying is not limited by the frequency diversity of the bottleneck relay link, thanks to the adopted link selection scheme. For example, if $d_{\text{f}} = 5$, $L_{SR} = 3$, and $L_{RD} = 1$, $G_d = 4G_d^{\text{AF/DF}}$ holds according to (29). In Section V, we validate the predicted diversity gain benefits of buffer–aided relaying by simulations.

On the other hand, for finite buffer size, we determine the diversity gain based on (22) as

$$G_d = \min\{r_{SR}, r_{RD}\} = \min\{d_{\text{f}}, L_{SR}, L_{RD}\}, \quad (30)$$

which is identical to the diversity gain of conventional DF and AF BICM–OFDM relaying [17], [14]. However, as $J$ increases, we observe considerable diversity benefits in the useful SNR region as will be shown in Section V.

## IV. Average Delay Analysis

The use of buffers at the relay improves the performance at the expense of a higher delay in the network. Hence, it is important to study the end–to–end delay to understand the performance–delay tradeoff of the proposed buffer–aided relaying scheme. In this section, we analyze the average delay of the proposed scheme. We provide a closed–form expression for the average delay in terms of the buffer size and the probabilities of selection of the links. Note that unlike some other buffer–aided relaying schemes, e.g. [9], the relay appends the packet to its queue regardless of whether there is a decoding error or not. Hence, the relay does not need to send any acknowledgment message.

Since we assume that the source has always data to transmit, i.e., it has an infinite backlog of information bits, the delay is caused only by the buffer at the relay. Let $T(i)$ and $Q(i)$ denote the delay of the packet transmitted by the source and the queue length in time slot $i$, respectively. According to Little's law [18], the average delay $T = \mathcal{E}\{T(i)\}$, which is the average time that a packet is stored in the relay buffer, is given by

$$T = \frac{Q}{R_A} \quad \text{time slots}, \quad (31)$$

where $Q=\mathcal{E}\{Q(i)\}$ (in packets) is the average queue length at the buffer and $R_A$ (in packets/slot) is the average arrival rate into the queue. We assume a fixed rate transmission model and both the source and the relay transmit at a constant instantaneous rate $R$ when they are selected for transmission. For simplicity and without loss of generality we assume that the transmitting node transmits one packet at each time slot, i.e., $R=1$ (packet/slot). We define the probabilities of selecting the $S \rightarrow R$ and $R \rightarrow D$ links according to the finite buffer size link selection criterion in Subsection II-B as $\tilde{P}_{SR}$ and $\tilde{P}_{RD}$, respectively. Then, the average arrival rate into the relay buffer is $R_A=\tilde{P}_{SR}R=\tilde{P}_{SR}$. Similarly, the average departure rate from the relay buffer is $R_D=\tilde{P}_{RD}R=\tilde{P}_{RD}$. Note that $P_Z$, $Z \in \{SR, RD\}$, denotes the probabilities of link selection based on (5) only, i.e., excluding the cases corresponding to empty and full buffer states.

For a buffer of size $J$, the average queue length can be expressed as

$$Q=\sum_{i=0}^{J} iP_{G_i} \tag{32}$$

where the probabilities of different buffer states, $P_{G_i}$, are introduced in (42). $P_{G_J}=P_{\text{full}}$ and $P_{G_0}=P_{\text{empty}}$ are provided in (57) and (58), respectively, and $P_{G_i}$ is obtained by solving the linear equations in (42) as

$$P_{G_i} \;=\; \frac{P_{RD}^{J-i-1}}{P_{SR}^{J-i}}P_{G_J}, \quad i=1,...,J-1. \tag{33}$$

Using (57), (58), and (33), and the following equality

$$\sum_{k=0}^{n-1} kD^k=\frac{D(1-D^{n-1})}{(1-D)^2}-\frac{(n-1)D^n}{1-D}, \quad D\neq 1,\; n>1, \tag{34}$$

we obtain

$$Q=\left(\frac{\left(\frac{P_{RD}}{P_{SR}}\right)^{J-1}-1}{P_{RD}\left(1-\frac{P_{SR}}{P_{RD}}\right)^2}-\frac{(J-1)}{P_{RD}\left(1-\frac{P_{SR}}{P_{RD}}\right)}+J\right)P_{G_J}. \tag{35}$$

Moreover, according to the link selection protocol for finite buffer size, the average arrival rate into the relay buffer can be obtained as

$$R_A=\tilde{P}_{SR}=\left(1-P_{G_J}\right)P_{SR}+P_{G_0}P_{RD}. \tag{36}$$

Finally, using (35) and (36) in (31), the closed-form expression of the average delay is obtained as

$$T=\frac{P_{G_J}}{\left(1-P_{G_J}\right)P_{SR}+P_{G_0}P_{RD}} \times\left(\frac{\left(\frac{P_{RD}}{P_{SR}}\right)^{J-1}-1}{P_{RD}\left(1-\frac{P_{SR}}{P_{RD}}\right)^2}-\frac{(J-1)}{P_{RD}\left(1-\frac{P_{SR}}{P_{RD}}\right)}+J\right). \tag{37}$$

It is worth noting that for the special case when $P_{SR}=P_{RD}$, i.e., $\rho=\frac{\mathcal{E}\{\gamma_{SR}\}}{\mathcal{E}\{\gamma_{RD}\}}$, we can show that

$$T=J, \tag{38}$$

that is, the delay is linear in the buffer size.

Let us now investigate the behavior of the average delay when the buffer size tends to infinity, i.e., $J\rightarrow\infty$. For this purpose, we consider three cases:
*Case 1* ($P_{SR}=P_{RD}$, i.e., $\rho=\frac{\mathcal{E}\{\gamma_{SR}\}}{\mathcal{E}\{\gamma_{RD}\}}$): From (38), we can see that for buffer size $J\rightarrow\infty$, the average delay is $T\rightarrow\infty$.
*Case 2* ($P_{SR}>P_{RD}$, i.e., $\rho<\frac{\mathcal{E}\{\gamma_{SR}\}}{\mathcal{E}\{\gamma_{RD}\}}$): For $J\rightarrow\infty$, it can be shown from (35) and (36) that the average queue length $Q\rightarrow\infty$ and the average arrival rate $R_A\approx\frac{P_{SR}}{1+P_{SR}-P_{RD}}$. Hence, in this case, the average delay is $T\rightarrow\infty$.
*Case 3* ($P_{SR}<P_{RD}$, i.e., $\rho>\frac{\mathcal{E}\{\gamma_{SR}\}}{\mathcal{E}\{\gamma_{RD}\}}$): For $J\rightarrow\infty$, using (35) and (36), and after some simplifications, it can be shown that

$$T=\frac{Q}{R_A}\approx\frac{1}{P_{RD}-P_{SR}}. \tag{39}$$

Based on the above delay analysis and the PEP analysis in Section III, we can see that both the upper bound on the PEP and the average delay depend on $\rho$ (and hence $P_{SR}$ and $P_{RD}$) and the buffer size $J$. More specifically, if we choose $\rho$ as in (24), we have $P_{SR}=P_{RD}$. For infinite buffer size, the diversity gain in this case is $G_d=r_{SR}+r_{RD}$, however, the average delay is infinite, cf. (39). To limit the average delay we need to starve the buffer which can be done by choosing $\rho>\frac{\mathcal{E}\{\gamma_{SR}\}}{\mathcal{E}\{\gamma_{RD}\}}$, but with this choice of $\rho$ the diversity gain becomes $G_d=r_{SR}$. Note that the closer the value of $\rho$ to $\frac{\mathcal{E}\{\gamma_{SR}\}}{\mathcal{E}\{\gamma_{RD}\}}$, the larger the average delay and the higher the diversity benefits in the practical SNR region. For the finite buffer size case and $\rho=\frac{\mathcal{E}\{\gamma_{SR}\}}{\mathcal{E}\{\gamma_{RD}\}}$, the average delay equals the buffer size, i.e., $T=J$, cf. (38), and the larger the buffer size the larger the average delay and the higher the diversity benefits in the practical SNR region, since $P_{\text{empty}}, P_{\text{full}}\rightarrow 0$ when $J\rightarrow\infty$. Hence, one way to limit the average delay is to decrease the buffer size but this is at the expense of the diversity gain in the practical SNR region. Another way to limit the average delay is by starving the buffer which can be done by choosing $\rho>\frac{\mathcal{E}\{\gamma_{SR}\}}{\mathcal{E}\{\gamma_{RD}\}}$. However, this choice also results in a loss of diversity gain in the practical SNR region since $P_{\text{empty}}$ does not tend to zero when $J\rightarrow\infty$. Hence, if a large delay can be tolerated, a large buffer size and $\rho=\frac{\mathcal{E}\{\gamma_{SR}\}}{\mathcal{E}\{\gamma_{RD}\}}$ result in optimum error rate performance. Therefore, to achieve a certain tradeoff between the diversity gain and the average delay, the designer has to choose appropriate values for $\rho$ and $J$. We will study the impact of $\rho$ and the buffer size $J$ on the diversity gain and average delay in more detail in Section V.

## V. Simulation Results

In this section, we present Monte–Carlo simulation results to investigate the impact of the various system and channel parameters on the performance of BICM–OFDM systems with a buffer–aided relay. Throughout this section, we adopt the standard rate $1/2$ convolutional code with generator polynomials $(7,5)_8$ and free distance $d_{\text{f}}=5$, Gray labeling, 16–QAM modulation, and $N_t=64$ sub–carriers of which $N=60$ are data sub–carriers. We assume source and relay employ the same channel code and transmit at fixed rate. We do not consider power allocation in this paper and assume that both source and relay transmit with equal power $P$. The interleaver

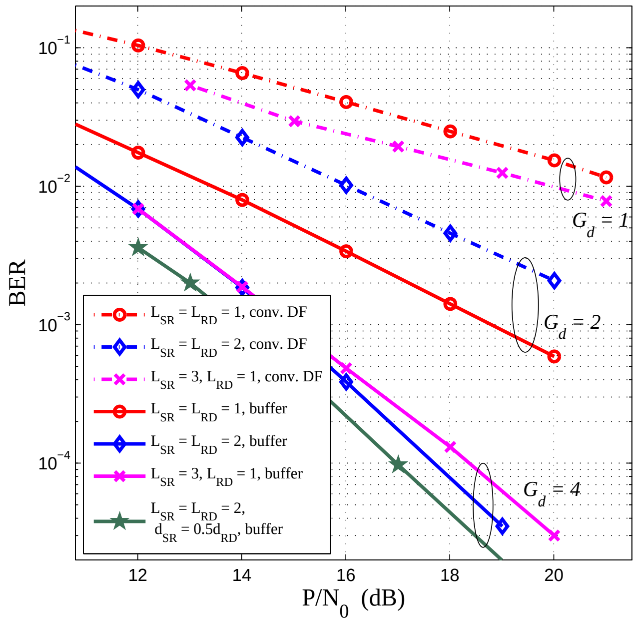


Fig. 2. BER vs. transmit SNR for BICM–OFDM system employing a relay which has a buffer of infinite size. Unless mentioned otherwise, we assume $d_{SR} = d_{RD}$.

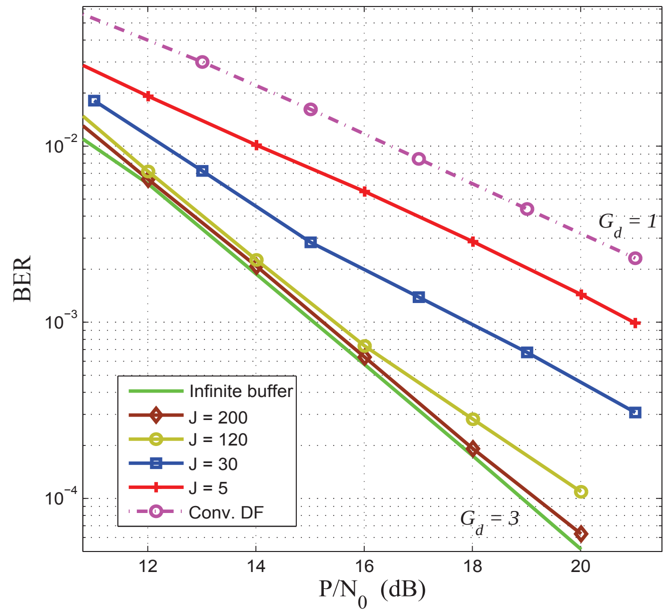


Fig. 3. BER vs. transmit SNR for BICM–OFDM system employing a relay with a buffer of finite size.

for BICM–OFDM is designed as outlined in [10]. The coefficients of the CIRs of all links are independent Rayleigh fading. The performance results are averaged over 1,000,000 independent channel realizations. Furthermore, the path–loss exponent is $\alpha = 2$. Unless mentioned otherwise, we adopt $\rho$ as shown in (26) assuming a uniform PDP. As is customary in the BICM–OFDM literature see e.g. [10], we validate the derived analytical results in terms of the diversity gain, since the PEPs in (22) and (27) are obtained via multiple upper bounding steps rendering the resulting coding gain loose. However, as the average delay expressions presented in Section IV are exact, we compare the corresponding simulation results with their analytical counterparts.

### A. BER Performance

First, we consider the diversity gain performance of the system for infinite buffer size. Fig. 2 shows the BER vs. transmit SNR ($P/N_0$) for different CIR lengths $L_{SR}$ and $L_{RD}$. Solid lines denote the performance of buffer–aided relaying and dashed lines denote the performance of conventional DF relaying. We observe that for buffer–aided (conventional DF) relaying for $L_{SR} = L_{RD} = 1$ and $L_{SR} = L_{RD} = 2$, the diversity gain is $G_d = 2$ ($G_d^{\mathrm{DF}} = 1$) and $G_d = 4$ ($G_d^{\mathrm{DF}} = 2$), respectively. We see that if both links have identical frequency diversity, buffer–aided relaying doubles the diversity gain. For $L_{SR} = 3$ and $L_{RD} = 1$, buffer–aided relaying yields a diversity gain of $G_d = 4$, whereas for conventional relaying, we have a diversity gain of $G_d^{\mathrm{DF}} = 1$ only, which is also supported by the diversity gain expression derived in Section III-B. Hence, buffer–aided relaying is not limited by the bottleneck link and results in a high diversity order for links with non–identical frequency diversity as well. Note that according to (26), we have $\rho = 1$ for the aforementioned cases. For non–identically distributed links with $L_{SR} = L_{RD} = 2$ and $d_{SR} = 0.5 d_{RD}$, we also observe $G_d = 4$. Here, $\rho = d_{RD}^2/d_{SR}^2 = 4$ holds according to (26) which compensates for the larger path–loss of the $R \to D$ link and ensures that the selection of the $S \to R$ and $R \to D$ links remains equally probable.

In Fig. 3, we show the BER vs. transmit SNR ($P/N_0$) for different buffer sizes $J$. We assume the relay buffer is empty when transmission starts. Here, we consider non–identically distributed links with $L_{SR} = 1$, $L_{RD} = 2$, and $d_{SR} = 0.5 d_{RD}$, i.e., $\rho = d_{RD}^2/d_{SR}^2 = 4$ holds. Solid lines denote the performance of buffer–aided relaying and the dashed line denotes the performance of conventional DF relaying. We observe that even with a small buffer size of $J = 5$, buffer–aided relaying results in a significant coding gain. As $J$ increases, we observe diversity gain benefits in the practical SNR region[5]. For $J = 200$, we obtain nearly identical performance as for infinite buffer size in the considered SNR region. Hence, in conclusion, buffers with moderate number of elements result in significant performance gains compared to conventional DF relaying confirming the potential of the scheme.

Since in time–variant channels the CSI used for link selection may be already outdated when transmission starts, we investigate next the impact of outdated CSI. To this end, we model the outdated sub–carrier channel gains of the $S \to R$ and $R \to D$ links used for link selection as [19]

$$\hat{H}_{SR}[k] = \beta_1 H_{SR}[k] + \sqrt{1-\beta_1^2}\, v_{SR}[k] \qquad (40)$$
$$\hat{H}_{RD}[k] = \beta_2 H_{RD}[k] + \sqrt{1-\beta_2^2}\, v_{RD}[k]$$

where $v_Z[k]$, $Z \in \{SR, RD\}$, are circularly symmetric complex Gaussian random variables having the same variance as

[5] The "practical" SNR region depends on the application. In this paper, we refer to the range of 10dB–20dB as the practical SNR region.

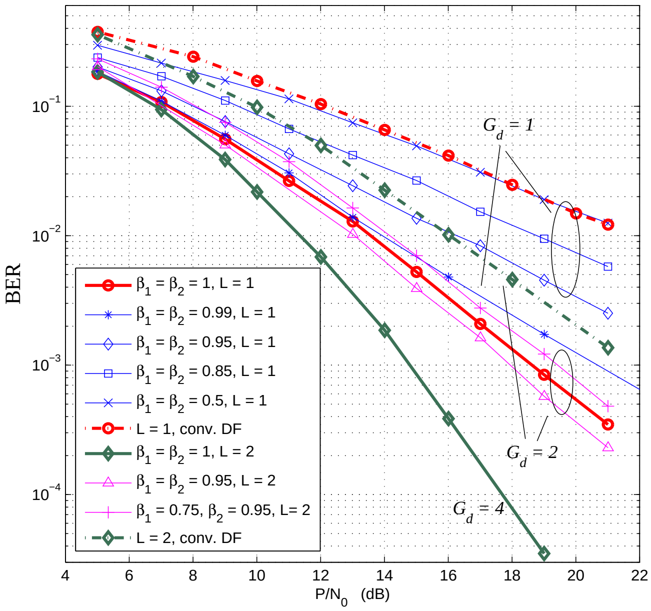


Fig. 4. BER vs. transmit SNR for outdated CSI. A relay with a buffer of infinite size is used and all links have identical frequency diversity $L$. Solid lines denote buffer–aided relaying and dashed lines denote conventional DF relaying.

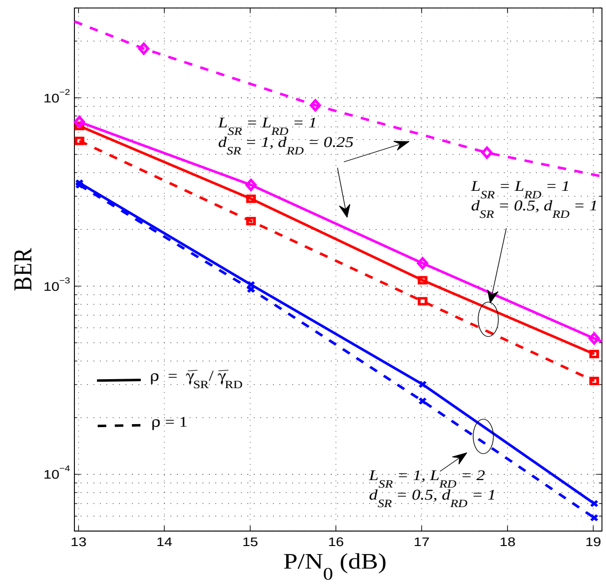


Fig. 5. BER vs. transmit SNR for BICM–OFDM system for different choices of the decision threshold $\rho$. A relay with a buffer of infinite size is employed.

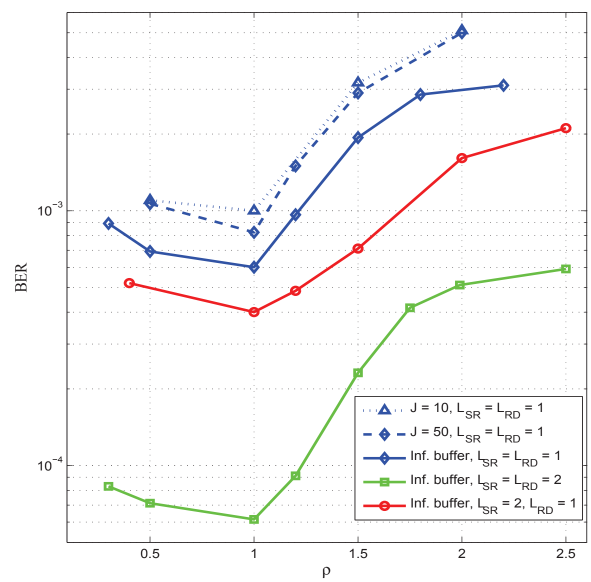


Fig. 6. BER vs. $\rho$ for both finite and infinite buffer size. We assume $d_{SR} = d_{RD}$ and i.i.d. links.

the current sub–carrier channel gains $H_Z[k]$, $v_Z[k]$ and $H_Z[k]$ are mutually independent, and $\beta_1$ ($\beta_2$) is the correlation coefficient between $\hat{H}_{SR}[k]$ and $H_{SR}[k]$ ($\hat{H}_{RD}[k]$ and $H_{RD}[k]$). Following Jakes' model, the correlation coefficients are given by $\beta_1 = J_0(2\pi f_{d,SR}T_d)$ ($\beta_2 = J_0(2\pi f_{d,RD}T_d)$) [20], $J_0(\cdot)$ denotes the zeroth order Bessel function of the first kind, $f_{d,Z}$ is the maximum Doppler frequency of link $Z$, and $T_d$ is the delay between (perfect) CSI estimation and transmission. For example, $f_{d,Z} = 50$ Hz (which corresponds to a carrier frequency of 1.8 GHz and a mobile terminal speed of 30 km/hr) for $T_d = \{640\ \mu s, 1.432\ ms, 2.514\ ms, 3.292\ ms\}$ leads to $\beta_i = \{0.99, 0.95, 0.85, 0.75\}$, respectively, cf. Fig. 4. From Fig. 4, we observe that for $L = L_{SR} = L_{RD} = 1$, the diversity gain reduces from $G_d = 2$ for perfect CSI (i.e., $\beta_1 = \beta_2 = 1$) to $G_d = 1$ for outdated CSI (i.e., $\beta_1 < 1$ and $\beta_2 < 1$). Similar observations can be made for $L = L_{SR} = L_{RD} = 2$, where outdated CSI reduces the achievable diversity gain from $G_d = 4$ to $G_d = 2$. Thus, if the CSI is outdated, the diversity gain advantage of buffer–aided relaying compared to conventional relaying disappears. This phenomenon is well known from other diversity mechanisms involving selection. For example, it has been shown in [19], [21] that the diversity gain of conventional relay selection disappears if the CSI is outdated. Nevertheless, Fig. 4 also reveals that buffer–aided relaying with adaptive link selection still achieves substantial performance gains compared to conventional relaying even if the CSI is severely outdated.

In Fig. 5, we compare the BERs for $\rho$ as in (26) and $\rho = 1$ for infinite buffer size. First, we consider the case when $\bar{\gamma}_{SR} > \bar{\gamma}_{RD}$. Here, we assume link distances $d_{RD} = 2d_{SR} = 1$, hence, the path–loss of the $R \to D$ link is larger than that of the $S \to R$ link. For $L_{SR} = L_{RD} = 1$ and $L_{SR} = 1$, $L_{RD} = 2$, we observe that $\rho = 1$ performs slightly better than $\rho$ from (26) and both achieve the same diversity. As buffer overflow never occurs because of the infinite buffer size, $\rho = 1$ always selects the link with the largest instantaneous SNR (cf. $\gamma_Z^t$ in Section II-B). The downside is that it will select the $S \to R$ link more often than the $R \to D$ link, which will cause a prohibitive delay for the transmitted packets. For example, for transmitting a fixed number of packets, say 1000 packets, from $S$ to $D$, 8335 channel uses are needed if $\rho$ is selected as in (26) compared to 32706 channel uses for $\rho = 1$ at a transmit SNR of 19 dB for $L_{SR} = 1$, $L_{RD} = 2$, and $d_{RD} = 2d_{SR} = 1$. Furthermore, we consider the case when $\bar{\gamma}_{SR} < \bar{\gamma}_{RD}$. We assume $L_{SR} = L_{RD} = 1$ and $d_{SR} = 4d_{RD} = 1$, hence, the path–loss in the $S \to R$ link is larger than that of the $R \to D$ link. In this case, $\rho = 1$ will select the $R \to D$ link more often. Hence, buffer underflow will occur with a high

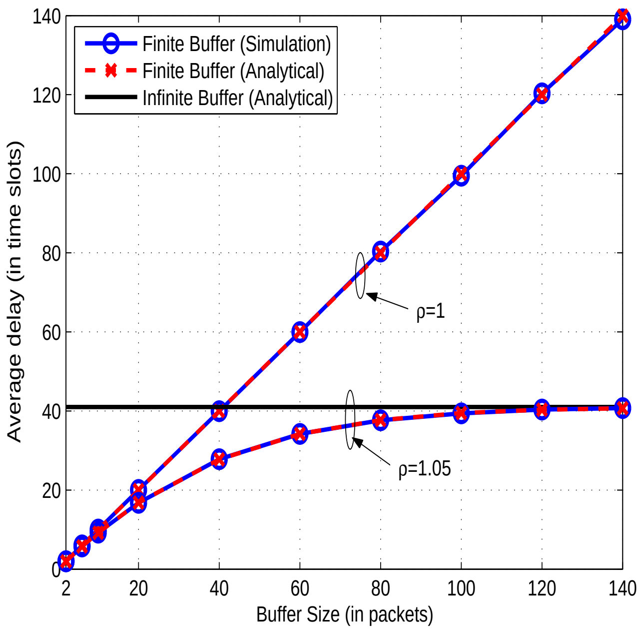


Fig. 7. Average delay vs. buffer size. Analytical and simulation results are shown. The analytical results were obtained from (37) , (38), and (39).

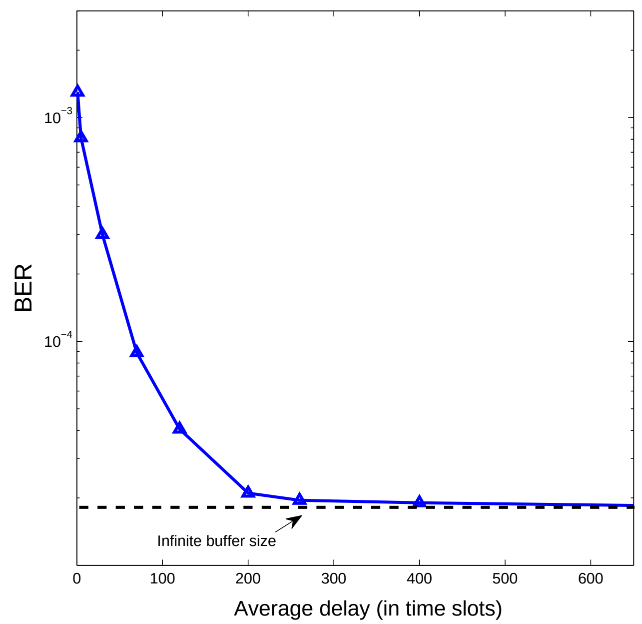


Fig. 8. BER vs. average delay for buffers of finite size. The dashed line refers to BER obtained with infinite buffer size.

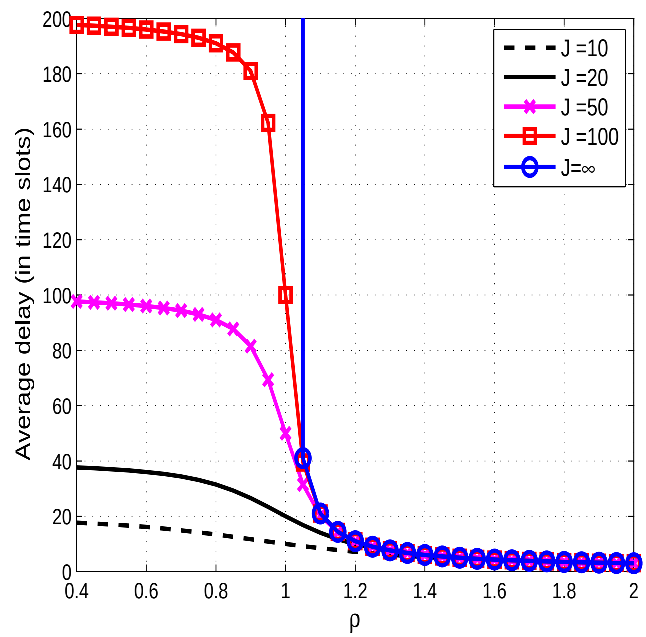


Fig. 9. Average delay vs. $\rho$.

probability and the relay will be forced to receive packets from the source more frequently. Hence, we observe a diversity loss for $\rho = 1$ when $\bar{\gamma}_{SR} < \bar{\gamma}_{RD}$. However, choosing $\rho$ according to (26) results in full diversity as it ensures that the links are selected with equal probability.

In Fig. 6, we show BER vs. $\rho$ for a transmit SNR of 20 dB for different link frequency diversities and different buffer sizes. As i.i.d. links are assumed, we observe that $\rho = 1$ results in the lowest BER in all cases.

### *B. Delay Performance*

In Fig. 7, we show the average delay for buffers of finite size for different values of $\rho$, where we compare simulation and analytical results. We assume the links are i.i.d. We adopt $\rho = 1.05 > 1$ to obtain a finite average delay for buffers with infinite size and use it as reference for the performance of buffers with finite size. We observe that as the buffer size increases, the average delay with finite buffer size gradually converges to that obtained with infinite buffer size. Furthermore, for $\rho = 1$, we observe that the average delay increases linearly as the buffer size increases, as expected. We also clearly see that the simulation and analytical results are in perfect agreement.

In Fig. 8, we show BER vs. average delay for i.i.d links with $L_{SR} = 2$ and $L_{RD} = 2$, and $d_{SR} = d_{RD}$, i.e., $\rho = 1$ holds. We observe that as the buffer size (i.e., delay) increases, the BER gradually converges to that obtained with infinite buffer size. Hence, in this example, we see that even moderate buffer sizes result in a similar performance as observed with infinite buffer size, and thus providing a profitable delay–BER tradeoff.

In Fig. 9, we show the average delay vs. $\rho$ for different buffer sizes. Again, we assume the links are i.i.d. We observe that as $J \to \infty$ and $\rho \to 1$, the average delay increases sharply and for $\rho = 1$ it tends to infinity. On the other hand, if we increase $\rho$, the average delay decreases as the $R \to D$ link is selected more often. However, this comes at the expense of a loss in BER performance as shown in Fig. 6 since the best link is not always chosen. The results in Figs. 6, 8, and 9 give insight into how to choose $\rho$ and the buffer size in order to obtain a certain average delay and BER performance tradeoff.

## VI. Conclusions

In this paper, we studied a BICM–OFDM system employing a relay which was equipped with a buffer of finite or infinite size. We proposed new link selection protocols for both finite and infinite buffer sizes. We performed a closed–form worst–case PEP analysis for the scheme and provided expressions for the diversity gain. We observed that remarkable performance gains can be obtained if relays are equipped with buffers. The analysis revealed that compared to conventional relaying, the diversity gain of the proposed link selection protocol is twice as large for links with identical frequency diversity and more than twice as large for links with non–identical frequency diversity because the bottleneck relay link does not limit the performance. Moreover, we analyzed the delay of the proposed scheme and obtained a closed-form expression for the average delay. The average delay analysis provided insight on how to choose $\rho$ and the buffer size to achieve a desired BER–delay tradeoff. Our results showed that for buffers of moderate size, significant coding gains can be achieved, if not any diversity gain.

## Appendix A
## Probabilities of Full and Empty Buffer

In this appendix, we derive the probabilities of the buffer being full and empty which are denoted by $P_{\text{full}}$ and $P_{\text{empty}}$, respectively. $P_{\text{full}}$ and $P_{\text{empty}}$ are provided in the following theorem.

*Theorem 1:* For a buffer of size $J$ and given the selection rule in Table I, where the $R \to D$ ($S \to R$) link is selected when the buffer is full (empty), we have

$$\begin{aligned} P_{\text{full}} &= \left[1 + \frac{1}{P_{SR}} \frac{\zeta^J - 1}{\zeta - 1} + \zeta^{J-1}\right]^{-1} \\ \text{and} \quad P_{\text{empty}} &= \zeta^{J-1} P_{\text{full}}, \end{aligned} \tag{41}$$

where $\zeta \triangleq \frac{P_{RD}}{P_{SR}}$, and $P_{SR} = \Pr(\gamma_{SR}^t > \rho\gamma_{RD}^t)$ and $P_{RD} = \Pr(\gamma_{RD}^t > \gamma_{SR}^t/\rho)$ are the probabilities for selection of the $S \to R$ and $R \to D$ links, respectively, based on (5).

*Proof:* In order to compute $P_{\text{empty}}$ and $P_{\text{full}}$, we model the possible states of the buffer and the transition between the states as a Markov chain.[6] For a buffer of size $J$, we have a Markov chain with $N_s = J + 1$ states. Let $G_i \triangleq i$, $i = 0, \cdots, J$, denote the $i$th state in the Markov chain, where $i$ represents the number of full elements in the buffer. Let $p_{m,n}$ denote the probability of transition from state $G_m$ to state $G_n$. Given the link selection protocol for the finite buffer case described in Section II-B, we have the following three cases:

1) If the buffer is in state $G_0$, i.e., the buffer is empty, the only possible transition is to state $G_1$ with probability $p_{0,1} = 1$. In this case, we enforce the selection of the $S \to R$ link.
2) If the buffer is in state $G_J$, i.e., the buffer is full, the only possible transition is to state $G_{J-1}$ with probability $p_{J,J-1} = 1$. In this case, we enforce the selection of the $R \to D$ link.
3) If the buffer is in state $G_i$, $i \in \{1, \ldots, J-1\}$, i.e., the buffer is neither empty nor full, there are two possible transitions. The first possible transition is from state $G_i$ to state $G_{i-1}$ with probability $p_{i,i-1} = P_{RD}$. The second possible transition is from state $G_i$ to state $G_{i+1}$ with probability $p_{i,i+1} = P_{SR}$. Note that $P_{SR} + P_{RD} = 1$ holds.

[6] We note that Markov chain models were used to analyze the performance of relay networks before. For example, in [7] a Markov chain model was adopted to analyze the outage performance of link selection in a multi–relay network.

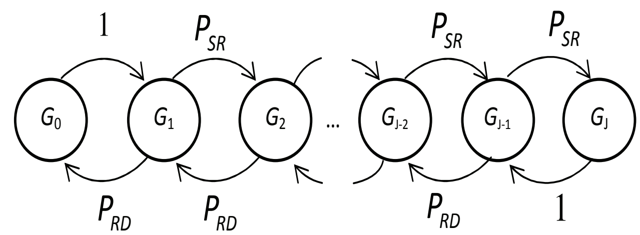


Fig. 10. State diagram of the Markov chain representing the states of the buffer in the relay.

Fig. 10 depicts the state diagram of the Markov chain representing the states of the buffer of the relay and the transitions between them. Let $P_{G_i}$ denote the probability of being in state $G_i$ Based on the state diagram in Fig. 10, we have

$$\begin{aligned} &P_{G_0} = p_{1,0} P_{G_1} = P_{RD} P_{G_1}, \\ &P_{G_1} = p_{0,1} P_{G_0} + p_{2,1} P_{G_2} = P_{G_0} + P_{RD} P_{G_2}, \\ &P_{G_i} = P_{RD} P_{G_{i+1}} + P_{SR} P_{G_{i-1}}, \quad 2 \le i \le J-2, \\ &P_{G_{J-1}} = P_{G_J} + P_{SR} P_{G_{J-2}}, \\ &P_{G_J} = P_{SR} P_{G_{J-1}}. \end{aligned} \tag{42}$$

Using the fact that $\sum_{i=0}^{J} P_{G_i} = 1$ and by solving the equations in (42), we obtain the expressions for $P_{\text{empty}} = P_{G_0}$ and $P_{\text{full}} = P_{G_J}$ as

$$\begin{aligned} P_{\text{full}} &= \left[1 + \sum_{i=0}^{J-2} \frac{P_{RD}^i}{P_{SR}^{i+1}} + \Big(\frac{P_{RD}}{P_{SR}}\Big)^{J-1}\right]^{-1} \\ \text{and} \quad P_{\text{empty}} &= \Big(\frac{P_{RD}}{P_{SR}}\Big)^{J-1} P_{\text{full}}. \end{aligned} \tag{43}$$

Eq. (41) is obtained by exploiting

$$\sum_{k=1}^{N} D^{k-1} = \frac{D^N - 1}{D - 1}, \quad D \ne 1. \tag{44}$$

This concludes the proof. ■

## Appendix B
## Proof of Lemma 1

In this appendix, we derive expressions for the worst–case link PEPs $P_R^1(\boldsymbol{c}, \hat{\boldsymbol{c}})$ and $P_D^1(\hat{\boldsymbol{c}}, \tilde{\boldsymbol{c}})$ given in (9) and (10), respectively. After dropping time index $t$, we can rewrite the numerator of the right hand side of (9) as

$$\begin{aligned} &\mathcal{E}\{\exp(-\eta\gamma_{SR}) \cap \gamma_{SR} > \rho\gamma_{RD}\} \\ &= \int_0^\infty \int_{\rho z}^\infty \exp(-\eta x) f_{\gamma_{SR}}(x) f_{\gamma_{RD}}(z)\, dx\, dz, \end{aligned} \tag{45}$$

where $f_{\gamma_Z}(x)$ is the probability density function (PDF) of $\gamma_Z$, $Z \in \{SR, RD\}$. Now, to evaluate (45), we need to calculate $f_{\gamma_Z}(x)$, $Z \in \{SR, RD\}$. This is done in Appendix C and exact and asymptotic expressions for $f_{\gamma_Z}(x)$ are provided in (55) and (56), respectively.

Now, from (45) and (55) in Appendix C, we obtain

$$\int_{\rho z}^{\infty} \exp(-\eta x) f_{\gamma_{SR}}(x) dx = \sum_{j=1}^{r_{SR}} \frac{\lambda_j^{r_{SR}-1}(\boldsymbol{B}_{SR}) \exp\Big(-\rho\Big(\eta + \frac{1}{\lambda_j(\boldsymbol{B}_{SR})\bar{\gamma}_{SR}}\Big) z\Big)}{(1+\lambda_j(\boldsymbol{B}_{SR})\bar{\gamma}_{SR}\eta)\prod_{k=1,k\neq j}^{r_{SR}}(\lambda_j(\boldsymbol{B}_{SR})-\lambda_k(\boldsymbol{B}_{SR}))}, \quad (46)$$

where $r_Z \triangleq \min(d_{\mathrm{f}}, L_Z)$ and constant (SNR independent) matrix $\boldsymbol{B}_Z$, $Z \in \{SR, RD\}$, is defined in (52). Using (45) and (46), we obtain $\mathcal{E}\{\exp(-\eta\gamma_{SR}) \cap \gamma_{SR} > \rho\gamma_{RD}\}$ in (47) at the top of next page. Furthermore, $\Pr(\gamma_{SR} > \rho\gamma_{RD})$ also needed in (9) can be expressed as

$$\Pr(\gamma_{SR} > \rho\gamma_{RD}) = \int_0^{\infty} \left(\int_{\rho z}^{\infty} f_{\gamma_{SR}}(x) dx\right) f_{\gamma_{RD}}(z) dz, \quad (48)$$

where $f_{\gamma_Z}(x)$, $Z \in \{SR, RD\}$, is again given by (55) in Appendix III. After evaluating the integral inside the parenthesis in (48), we have

$$\Pr(\gamma_{SR} > \rho\gamma_{RD}) = \int_0^{\infty} \sum_{j=1}^{r_{SR}} \frac{\lambda_j^{r_{SR}-1}(\boldsymbol{B}_{SR}) \exp(-\frac{\rho z}{\lambda_j(\boldsymbol{B}_{SR})\bar{\gamma}_{SR}})}{\prod_{k=1,k\neq j}^{r_{SR}}(\lambda_j(\boldsymbol{B}_{SR})-\lambda_k(\boldsymbol{B}_{SR}))} f_{\gamma_{RD}}(z) dz. \quad (49)$$

Evaluating (49), we obtain $\Pr(\gamma_{SR} > \rho\gamma_{RD})$ in (50) at the top of next page. We observe from (50) that $\Pr(\gamma_{SR} > \rho\gamma_{RD})$, i.e., the probability of selecting the $S \to R$ link based on (5), is a constant and does not scale with SNR but depends on $\rho$ and the eigenvalues of $\boldsymbol{B}_Z$. Thus, for $e\overline{\gamma}_{SR} = f\overline{\gamma}_{RD} = \overline{\gamma}_b$, the right hand side of (50) is independent of $\overline{\gamma}_b$. To determine how $P_R^1(\boldsymbol{c}, \hat{\boldsymbol{c}})$ behaves at high SNR, we obtain an asymptotic expression for $\mathcal{E}\{\exp(-\eta\gamma_{SR}) \cap \gamma_{SR} > \rho\gamma_{RD}\}$. To this end, we resort to the asymptotic PDF based approach proposed in [22] and exploit (56) in Appendix III to obtain an asymptotic upper bound for $\mathcal{E}\{\exp(-\eta\gamma_{SR}) \cap \gamma_{SR} > \rho\gamma_{RD}\}$ in (51) at the top of next page. Combining now (9), (50), and (51), we obtain for $P_R^1(\boldsymbol{c}, \hat{\boldsymbol{c}})$ the asymptotic upper bound given in (11). Using a similar approach, the asymptotic upper bound given in (12) for $P_D^1(\hat{\boldsymbol{c}}, \tilde{\boldsymbol{c}})$ can be obtained.

## Appendix C
## Derivation of $f_{\gamma_Z}(x)$

In this appendix, we derive exact and asymptotic expressions for the PDF of $\gamma_Z$, $f_{\gamma_Z}(x)$, $Z \in \{SR, RD\}$. Here, $\gamma_Z = \sum_{k\in\mathcal{K}_Z} \gamma_Z[k] = \bar{\gamma}\sum_{k\in\mathcal{K}_Z} |H_Z[k]|^2$, where $|\mathcal{K}_Z| = d_{\mathrm{f}}$ and $|H_Z[k]|^2 = |\boldsymbol{w}_Z^H[k]\boldsymbol{P}_Z\boldsymbol{h}_Z|^2$. Each element of $\boldsymbol{P}_Z\boldsymbol{h}_Z$ is zero mean complex Gaussian with variance $\sigma_{h_Z}^2$. Then, $\gamma_Z$ can be expressed as

$$\gamma_Z = \bar{\gamma}\boldsymbol{h}_Z^H \underbrace{\boldsymbol{P}_Z\boldsymbol{A}_Z\boldsymbol{P}_Z}_{\boldsymbol{B}_Z} \boldsymbol{h}_Z = \bar{\gamma}\boldsymbol{h}_Z^H\boldsymbol{V}_Z\boldsymbol{\Delta}_Z\boldsymbol{V}_Z^H\boldsymbol{h}_Z, \quad (52)$$

where $\boldsymbol{V}_Z\boldsymbol{\Delta}_Z\boldsymbol{V}_Z^H$ is the EVD of $\boldsymbol{B}_Z$, and $\boldsymbol{A}_Z = \sum_{k\in\mathcal{K}_Z}\boldsymbol{w}_Z[k]\boldsymbol{w}_Z^H[k]$. Let $v_Z(i)$ denote the $i$th element of vector $\boldsymbol{V}_Z^H\boldsymbol{h}_Z$. Then, $\gamma_Z = \bar{\gamma}\sum_{i=1}^{r_Z}\lambda_i(\boldsymbol{B}_Z)|v_Z(i)|^2$, where $\lambda_i(\boldsymbol{B}_Z)$ is the $i$th non–zero eigenvalue of $\boldsymbol{B}_Z$ and $r_Z$ is the rank of $\boldsymbol{B}_Z$ which is given by $\min(d_{\mathrm{f}}, L_Z)$ [10]. Now, the PDF of $\bar{\gamma}\lambda_i(\boldsymbol{B}_Z)|v_Z(i)|^2$ is given by $(1/(\bar{\gamma}\lambda_i(\boldsymbol{B}_Z)\sigma_{h_Z}^2))\exp(-x/(\bar{\gamma}\lambda_i(\boldsymbol{B}_Z)\sigma_{h_Z}^2))=(1/(\lambda_i(\boldsymbol{B}_Z)\bar{\gamma}_Z))\exp(-x/(\lambda_i(\boldsymbol{B}_Z)\bar{\gamma}_Z))$ and the corresponding moment generating function is given by $1/(1-\lambda_i(\boldsymbol{B}_Z)\bar{\gamma}_Z s)$. In general form, the PDF of $\gamma_Z$ is given by [23]

$$f_{\gamma_Z}(x) = \frac{1}{2\pi j}\int_{c-j\infty}^{c+j\infty}\left(\prod_{i=1}^{r_Z}\frac{1}{1-\lambda_i(\boldsymbol{B}_Z)\bar{\gamma}_Z s}\right)\exp\{-sx\}\mathrm{d}s. \quad (53)$$

Calculating (53) and following [24], we obtain

$$f_{\gamma_Z}(x) = \left[\prod_{i=1}^{r_Z}\frac{1}{(\lambda_i(\boldsymbol{B}_Z)\bar{\gamma}_Z)^i}\right] \times \sum_{j=1}^{r_Z}\frac{\exp(-\frac{x}{\lambda_j(\boldsymbol{B}_Z)\bar{\gamma}_Z})}{\prod_{k=1,k\neq j}^{r_Z}(\frac{1}{\lambda_k(\boldsymbol{B}_Z)\bar{\gamma}_Z}-\frac{1}{\lambda_j(\boldsymbol{B}_Z)\bar{\gamma}_Z})}. \quad (54)$$

After some manipulations, we arrive at

$$f_{\gamma_Z}(x) = \frac{1}{\bar{\gamma}_Z}\sum_{j=1}^{r_Z}\frac{\lambda_j^{r_Z-2}(\boldsymbol{B}_Z)\exp(-\frac{x}{\lambda_j(\boldsymbol{B}_Z)\bar{\gamma}_Z})}{\prod_{k=1,k\neq j}^{r_Z}(\lambda_j(\boldsymbol{B}_Z)-\lambda_k(\boldsymbol{B}_Z))}. \quad (55)$$

Note that the $\lambda_i(\boldsymbol{B}_Z)$, $i \in \{1,\ldots,r_Z\}$, are distinct[7] and $\lambda_j(\boldsymbol{B}_Z) - \lambda_k(\boldsymbol{B}_Z) \neq 0$, $j \neq k$, holds in (55). Following the approach in [22] for $\bar{\gamma}_Z \to \infty$, an asymptotic PDF for $\gamma_Z$ can be obtained as

$$f_{\gamma_Z}(x) \doteq \frac{1}{\Gamma(r_Z)\bar{\gamma}_Z^{r_Z}\prod_{l=1}^{r_Z}\lambda_l(\boldsymbol{B}_Z)}x^{r_Z-1}. \quad (56)$$

## Appendix D
## Proof of Lemma 2

In this appendix, we provide the proof for *Lemma* 2. We use the expressions for $P_{\text{full}}$ and $P_{\text{empty}}$ provided in (41) in *Theorem* 1 and consider three cases: $\zeta = 1$ ($P_{RD} = P_{SR}$) , $\zeta > 1$ ($P_{RD} > P_{SR}$), and $\zeta < 1$ ($P_{RD} < P_{SR}$).

*Case* 1 ($\zeta = 1$): It can be easily shown from (41) that, for $\zeta = 1$, $P_{\text{empty}}, P_{\text{full}} \to 0$ when $J \to \infty$. Hence, $P_{SR} = P_{RD} = \frac{1}{2}$ holds since $P_{SR} + P_{RD} = 1$.

*Case* 2 ($\zeta > 1$): In this case, we obtain $P_{\text{full}}$ from (41) as

$$P_{\text{full}} = \left[\frac{P_{RD}-P_{SR}-1}{P_{RD}-P_{SR}} + \frac{P_{RD}-P_{SR}+1}{P_{RD}-P_{SR}}\zeta^{J-1}\right]^{-1}. \quad (57)$$

As $J \to \infty$, $\zeta^{J-1} \to \infty$, and $P_{\text{full}} \to 0$ holds. However, we obtain $P_{\text{empty}}$ as

$$P_{\text{empty}} = \zeta^{J-1}\left[\frac{P_{RD}-P_{SR}-1}{P_{RD}-P_{SR}} + \frac{P_{RD}-P_{SR}+1}{P_{RD}-P_{SR}}\zeta^{J-1}\right]^{-1} = \left[\frac{P_{RD}-P_{SR}-1}{P_{RD}-P_{SR}}\zeta^{-(J-1)} + \frac{P_{RD}-P_{SR}+1}{P_{RD}-P_{SR}}\right]^{-1}. \quad (58)$$

From (58), it is clear that as $J \to \infty$, $P_{\text{empty}} \to \frac{P_{RD}-P_{SR}}{P_{RD}-P_{SR}+1} \neq 0$.

[7] Independent eigenvectors correspond to repeated eigenvalues only when the matrix is a scalar multiple of an identity matrix. As $\boldsymbol{A}_Z$ is not diagonal in nature, its non–zero eigenvalues are distinct.

$$\mathcal{E}\{\exp(-\eta\gamma_{SR})\cap\gamma_{SR}>\rho\gamma_{RD}\} = \sum_{j=1}^{r_{SR}}\sum_{i=1}^{r_{RD}}\Bigg[\frac{\lambda_j^{r_{SR}}(\boldsymbol{B}_{SR})\lambda_i^{r_{RD}-1}(\boldsymbol{B}_{RD})\bar{\gamma}_{SR}}{(1+\lambda_j(\boldsymbol{B}_{SR})\bar{\gamma}_{SR}\eta)(\lambda_j(\boldsymbol{B}_{SR})\bar{\gamma}_{SR}+(1+\lambda_j(\boldsymbol{B}_{SR})\bar{\gamma}_{SR}\eta)\rho\lambda_i(\boldsymbol{B}_{RD})\bar{\gamma}_{RD})} \times \frac{1}{[\prod_{k=1,k\neq j}^{r_{SR}}(\lambda_j(\boldsymbol{B}_{SR})-\lambda_k(\boldsymbol{B}_{SR}))][\prod_{p=1,p\neq i}^{r_{RD}}(\lambda_i(\boldsymbol{B}_{RD})-\lambda_p(\boldsymbol{B}_{RD}))]}\Bigg] \tag{47}$$

$$\Pr(\gamma_{SR}>\rho\gamma_{RD}) = \sum_{j=1}^{r_{SR}}\sum_{i=1}^{r_{RD}}\frac{\lambda_j^{r_{SR}}(\boldsymbol{B}_{SR})\lambda_i^{r_{RD}-1}(\boldsymbol{B}_{RD})\bar{\gamma}_{SR}}{(\lambda_j(\boldsymbol{B}_{SR})\bar{\gamma}_{SR}+\rho\lambda_i(\boldsymbol{B}_{RD})\bar{\gamma}_{RD})[\prod_{k=1,k\neq j}^{r_{SR}}(\lambda_j(\boldsymbol{B}_{SR})-\lambda_k(\boldsymbol{B}_{SR}))][\prod_{p=1,p\neq i}^{r_{RD}}(\lambda_i(\boldsymbol{B}_{RD})-\lambda_p(\boldsymbol{B}_{RD}))]} \tag{50}$$

$$\mathcal{E}\{\exp(-\eta\gamma_{SR})\cap\gamma_{SR}>\rho\gamma_{RD}\} \le \frac{\Gamma(r_{SR}+r_{RD})}{r_{RD}\Gamma(r_{SR})\Gamma(r_{RD})\rho^{r_{RD}}\bar{\gamma}_{SR}^{r_{SR}}\bar{\gamma}_{RD}^{r_{RD}}\eta^{r_{SR}+r_{RD}}\left[\prod_{j=1}^{r_{SR}}\lambda_j(\boldsymbol{B}_{SR})\right]\left[\prod_{i=1}^{r_{RD}}\lambda_i(\boldsymbol{B}_{RD})\right]} \tag{51}$$

*Case* 3 ($\zeta < 1$): Using a similar approach as in Case 2, we can show that for $J \to \infty$, $P_{\text{full}} \to \frac{P_{RD}-P_{SR}}{P_{RD}-P_{SR}-1} \neq 0$ and $P_{\text{empty}} \to 0$.

Hence, $P_{\text{empty}}, P_{\text{full}} \to 0$ when $J \to \infty$ is achieved if and only if $\zeta = 1$. This concludes the proof.

## References


[1] A. Sendonaris, E. Erkip, and B. Aazhang, "User Cooperation Diversity – Parts I and II," *IEEE Trans. Commun.*, vol. 51, pp. 1927–1948, Nov. 2003.

[2] B. Xia, Y. Fan, J. Thompson, and H. V. Poor, "Buffering in a Three Node Relay Network," *IEEE Trans. Wireless Commun.*, vol. 7, pp. 4492–4496, Nov. 2008.

[3] L. Ding, M. Tao, F. Yang, and W. Zhang, "Joint Scheduling and Relay Selection in One– and Two–Way relay Networks with Buffering," in *Proc. IEEE ICC*, Dresden, Germany, 2009.

[4] R. Wang, V. K. Lau, and H. Huang, "Opportunistic Buffered Decode–Wait–and–Forward (OBDWF) Protocol for Mobile Wireless Relay Networks," *IEEE Trans. Wireless Commun.*, vol. 10, pp. 1224–1231, Apr. 2011.

[5] N. Zlatanov, R. Schober, and P. Popovski, "Buffer–Aided Relaying with Adaptive Link Selection," *IEEE J. Select. Areas Commun.*, vol. 31, pp. 1530–1542, Aug. 2013.

[6] H. Liu, P. Popovski, E. de Carvalho, and Y. Zhao, "Sum–Rate Optimization in a Two-Way Relay Network with Buffering," *IEEE Commun. Lett.*, vol. 17, pp. 95–98, 2013.

[7] I. Krikidis, T. Charalambous, and J. S. Thompson, "Buffer–Aided Relay Selection for Cooperative Diversity Systems without Delay Constraints," *IEEE Trans. Wireless Commun.*, vol. 11, pp. 1957–1967, May 2012.

[8] A. Ikhlef, D. S. Michalopoulos, and R. Schober, "Max–Max Relay Selection for Relays with Buffers," *IEEE Trans. Wireless Commun.*, vol. 11, pp. 1124–1135, Mar. 2012.

[9] N. B. Mehta, V. Sharma, and G. Bansal, "Performance Analysis of a Cooperative System with Rateless Codes and Buffered Relays," *IEEE Trans. Wireless Commun.*, vol. 10, pp. 1069–1081, Apr. 2011.

[10] E. Akay and E. Ayanoglu, "Achieving Full Frequency and Space Diversity in Wireless Systems via BICM, OFDM, STBC, and Viterbi Decoding," *IEEE Trans. Commun.*, vol. 54, pp. 2164–2172, Dec. 2006.

[11] G. Caire, G. Taricco, and E. Biglieri, "Bit–Interleaved Coded Modulation," *IEEE Trans. Inform. Theory*, vol. 44, pp. 927–946, May 1998.

[12] U. Wachsmann, R. F. H. Fischer, and J. B. Huber, "Multilevel Codes: Theoretical Concepts and Practical Design Rules," *IEEE Trans. Inform. Theory*, vol. 45, pp. 1361–1391, Jul. 1999.

[13] T. Wang, A. Cano, G. B. Giannakis, and J. N. Laneman, "High-Performance Cooperative Demodulation with Decode-and-Forward Relays," *IEEE Trans. Commun.*, vol. 55, pp. 1427– 1438, Jul. 2007.

[14] T. Islam, A. Nasri, R. Schober, and R. K. Mallik, "Analysis and Relay Placement for DF Cooperative BICM–OFDM Systems," in *Proceedings of IEEE WCNC'11*, Cancun, Mexico, Mar. 2011.

[15] N. Zlatanov, R. Schober, and P. Povoski, "Throughput and Diversity Gain of Buffer Aided Relaying," in *Proc. IEEE GLOBECOM*, Houston, TX, Dec. 2011.

[16] N. Zlatanov and R. Schober, "Buffer–Aided Relaying with Adaptive Link Selection – Fixed and Mixed Rate Transmission," *IEEE Trans. Inform. Theory*, vol. 59, pp. 2816–2840, May 2013.

[17] T. Islam, R. Schober, R. K. Mallik, and V. K. Bhargava, "Analysis and Design of Cooperative BICM–OFDM Systems," *IEEE Trans. Commun.*, vol. 59, pp. 1742–1751, Jun. 2011.

[18] J. D. C. Little, "A Proof of the Queueing Formula: $L = \lambda w$," *Operations Research*, vol. 9, no. 3, pp. 383–388, 1961.

[19] J. L. Vicario, A. Bel, J. A. Lopez-Salcedo, and G. Seco, "Opportunistic Relay Selection with Outdated CSI: Outage Probability and Diversity Analysis," *IEEE Trans. Wireless Commun.*, vol. 8, pp. 2872–2876, Jun. 2009.

[20] E. W. C. Jakes, Jr., *Microwave Mobile Communications*. New Jersey: Prentice–Hall, 1974.

[21] D. S. Michalopoulos, H. A. Suraweera, G. K. Karagiannidis, and R. Schober, "Amplify–and–Forward Relay Selection with Outdated Channel Estimates," *IEEE Trans. Commun.*, vol. 60, pp. 1278– 1290, Jun. 2012.

[22] Z. Wang and G. Giannakis, "A Simple and General Parameterization Quantifying Performance in Fading Channels," *IEEE Trans. Commun.*, vol. 51, pp. 1389–1398, Aug. 2003.

[23] A. Papoulis, *Probability, Random Variables and Stochastic Processes*. Tokyo: McGraw–Hill, 1965.

[24] S. M. Ross, *Probability Models*. Amsterdam: Academic, 2003.



**Toufiqul Islam (S'10)** received his B.Sc. and M.Sc. degrees in Electrical and Electronic Engineering from Bangladesh University of Engineering and Technology, Dhaka, Bangladesh, in 2006 and 2008, respectively. Currently, he is working toward Ph.D. degree in Electrical and Computer Engineering at The University of British Columbia (UBC), Vancouver, Canada under joint supervision of Robert Schober and Vijay Bhargava.

His research interests include wireless network coding, buffer–aided relaying, interference alignment, and applications of machine learning techniques in communications. He has won the Donald N. Byers Prize, the highest graduate student honor at UBC. He was also the recipient of the prestigious Vanier Canada Graduate Scholarship, the Killam Doctoral Fellowship, and the UBC Four Year Fellowship in 2011, 2010, and 2009, respectively. Sponsored by a competitive German Academic Exchange Service (DAAD) research grant and the NSERC Michael Smith Foreign Study Supplements program, he visited the Institute of Digital Communications at the Friedrich Alexander University (FAU), Erlangen, Germany during the Summer of 2013. His paper was awarded 2nd prize in the IEEE Region 10 undergraduate student paper contest in 2006. He also won the IEEE Globecom 2012 travel grant award.

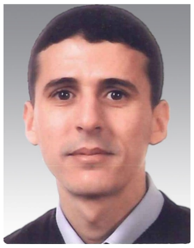

**Aissa Ikhlef** (M'09) was born in Constantine, Algeria. He received the B.S. degree in electrical engineering from the University of Constantine, Constantine, Algeria, in 2001 and the M.Sc. and Ph.D. degrees in electrical engineering from the University of Rennes 1, Rennes, France, in 2004 and 2008, respectively.

From 2004 to 2008, he was with Supélec, France, pursuing his Ph.D. degree. From 2007 to 2008, he was a lecturer at the University of Rennes 1. From 2008 to 2010 he was a Postdoctoral Fellow with the Communication and Remote Sensing Laboratory, Catholic University of Louvain, Louvain La Neuve, Belgium. He was a visiting Postdoctoral Fellow at the University of British Columbia, Vancouver, BC, Canada, from August to November 2009. From 2010 to 2013 he was with the data communications group, University of British Columbia, Vancouver, Canada, as a Postdoctoral Fellow. Since June 2013 he has been with Toshiba Research Europe Limited, Bristol, UK, as a Research Engineer. His current research interests include wireless communications and networking with emphasis on distributed beamforming and diversity techniques in cooperative communications.

**Robert Schober (M'01, SM'08, F'10)** was born in Neuendettelsau, Germany, in 1971. He received the Diplom (Univ.) and the Ph.D. degrees in electrical engineering from the University of Erlangen–Nuermberg in 1997 and 2000, respectively. From May 2001 to April 2002 he was a Postdoctoral Fellow at the University of Toronto, Canada, sponsored by the German Academic Exchange Service (DAAD). Since May 2002 he has been with the University of British Columbia (UBC), Vancouver, Canada, where he is now a Full Professor and Canada Research Chair (Tier II) in Wireless Communications. Since January 2012, he is an Alexander von Humboldt Professor and the Chair for Digital Communication at the Friedrich Alexander University (FAU), Erlangen, Germany. His research interests fall into the broad areas of Communication Theory, Wireless Communications, and Statistical Signal Processing.

Dr. Schober received several awards for his work including the 2002 Heinz Maier–Leibnitz Award of the German Science Foundation (DFG), the 2004 Innovations Award of the Vodafone Foundation for Research in Mobile Communications, the 2006 UBC Killam Research Prize, the 2007 Wilhelm Friedrich Bessel Research Award of the Alexander von Humboldt Foundation, the 2008 Charles McDowell Award for Excellence in Research from UBC, a 2011 Alexander von Humboldt Professorship, and a 2012 NSERC E. W. R. Steacie Fellowship. In addition, he received best paper awards from the German Information Technology Society (ITG), the European Association for Signal, Speech and Image Processing (EURASIP), IEEE WCNC 2012, IEEE Globecom 2011, IEEE ICUWB 2006, the International Zurich Seminar on Broadband Communications, and European Wireless 2000. Dr. Schober is a Fellow of the IEEE, the Canadian Academy of Engineering, and the Engineering Institute of Canada. He is currently the Editor–in–Chief of the IEEE TRANSACTIONS ON COMMUNICATIONS.

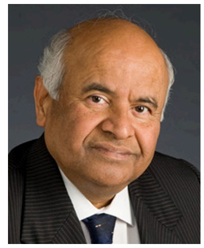

**Vijay K. Bhargava (M'74, SM'82, F'92)** is a Professor in the Department of Electrical and Computer Engineering at the University of British Columbia in Vancouver, where he served as Department Head from 2003–2008. From 1984 to 2013 he was with the University of Victoria where he served as the founding Graduate Advisor. From 1976 to 1984, he was with Concordia University in Montreal where he served as an undergraduate advisor and as the IEEE Student Branch Counselor. An active researcher, Vijay is currently leading a major R&D program in Cognitive and Cooperative Wireless Communication Networks. He received his PhD from Queen's University in 1974, and he appears on ISIHighlyCited.com as an *Institute of Scientific Information Highly Cited Researcher*. He is a Fellow of the IEEE, the Royal Society of Canada, the Engineering Institute of Canada, and the Engineering Institute of Canada.

Vijay is a co-author (with D. Haccoun, R. Matyas and P. Nuspl) of "Digital Communications by Satellite" (New York: Wiley: 1981), which has been translated to Chinese and Japanese. He is a co-editor (with S. Wicker) of "Reed Solomon Codes and their Applications" (IEEE Press: 1994), a co-editor (with V. Poor, V. Tarokh and S. Yoon) of "Communications, Information and Network Security" (Kluwer: 2003), a co-editor (with E. Hossain) of "Cognitive Wireless Communication Networks" (Springer: 2007), a co-editor (with E. Hossain and D. I. Kim) of "Cooperative Wireless Communications Networks" (Cambridge University Press: 2011), and a co-editor (with E. Hossain and G. Fettweis) of "Green Radio Communications Networks" (Cambridge University Press: 2012).

Vijay has played a major role in the creation of the IEEE Communications and Networking Conference (WCNC) and the IEEE TRANSACTIONS ON WIRELESS COMMUNICATIONS for which he served as the Editor–in–Chief during 2007–2009. He is a past President of the IEEE Information Theory Society, and is currently serving as the President of the IEEE Communications Society.